OPEN ACCESS
International Journal of Bifurcation and Chaos, Vol. 33, No. 10 (2023) 2350115 (25 pages)

DOI: 10.1142/S0218127423501158

Convergence of Discrete-Time Cellular Neural Networks with Application to Image Processing

Mauro Di Marco*, Mauro Forti† and Luca Pancioni‡
Department of Information Engineering and Mathematics,
University of Siena, Via Roma 56-53100 Siena, Italy
**dimarco@diism.unisi.it*
†*forti@diism.unisi.it*
‡*pancioni@diism.unisi.it*

Alberto Tesi
Department of Information Engineering,
University of Florence,
Via S. Marta 3-50139 Firenze, Italy
alberto.tesi@unifi.it

Received July 20, 2023

The paper considers a class of discrete-time cellular neural networks (DT-CNNs) obtained by applying Euler's discretization scheme to standard CNNs. Let T be the DT-CNN interconnection matrix which is defined by the feedback cloning template. The paper shows that a DT-CNN is convergent, i.e. each solution tends to an equilibrium point, when T is symmetric and, in the case where $T + E_n$ is not positive-semidefinite, the step size of Euler's discretization scheme does not exceed a given bound (E_n is the $n \times n$ unit matrix). It is shown that two relevant properties hold as a consequence of the local and space-invariant interconnecting structure of a DT-CNN, namely: (1) the bound on the step size can be easily estimated via the elements of the DT-CNN feedback cloning template only; (2) the bound is independent of the DT-CNN dimension. These two properties make DT-CNNs very effective in view of computer simulations and for the practical applications to high-dimensional processing tasks. The obtained results are proved via Lyapunov approach and LaSalle's Invariance Principle in combination with some fundamental inequalities enjoyed by the projection operator on a convex set. The results are compared with previous ones in the literature on the convergence of DT-CNNs and also with those obtained for different neural network models as the Brain-State-in-a-Box model. Finally, the results on convergence are illustrated via the application to some relevant 2D and 1D DT-CNNs for image processing tasks.

Keywords: Cellular neural network; convergence; discrete-time neural network; LaSalle's Invariance Principle.

†Author for correspondence

1. Introduction

The standard Cellular Neural Networks (CNNs) introduced by Chua and Yang [1988a, 1988b] have been one of the most investigated neural paradigms in the last decades. One main reason is that, due to the local and space-invariant interconnecting structure, which is defined via feedback and input (control) cloning templates, a CNN lends itself to an advantageous hardware implementation with respect to other neural paradigms as the Hopfield neural networks [Hopfield, 1984]. We refer the reader to [Roska *et al.*, 2006; Shi *et al.*, 2004; Roska *et al.*, 2009; Chua & Roska, 2005] for the main theoretic results and applications of the CNN paradigm.

The standard CNNs are a Continuous-Time (CT) neural network model described by a system of nonlinear differential equations. Although less investigated, discrete-time (DT) models of CNNs, which are described by nonlinear maps, play an important role in the theory and application. Harrer and Nossek [1992]; Harrer *et al.* [1992] were the first authors to introduce a synchronous DT version of CNNs considering both the case where the activations are binary discontinuous functions, or otherwise, they are smooth three-segment piecewise-linear function as in the standard CT-CNN model. Variants of DT-CNNs are studied by several authors (see, e.g. [Brucoli *et al.*, 1995; Chen *et al.*, 2014; Hänggi & Moschytz, 2000; Ding & Wang, 2020]). In particular, Chen and Shih [2004] have considered a synchronous DT-CNN model obtained by applying a forward Euler's discretization scheme to CT-CNNs. Generally speaking, DT-CNNs have the advantage with respect to CT-CNNs that they can be effectively implemented in digital hardware and they also allow for direct computer simulations of their dynamical behavior. In [Harrer *et al.*, 1992] it is also shown that DT-CNNs for image processing and pattern recognition tasks can be advantageously implemented using a dedicated analog electronic hardware. It is worth to mention that there are other relevant DT neural network models that have relationships with the DT-CNN model. For instance, the original DT Hopfield neural network [Hopfield, 1982] is described by an algorithm where the state of the neurons is asynchronously updated depending upon whether a linear combination of the states exceeds or not a given threshold. Moreover, the Brain-State-in-a-Box model introduced by Anderson *et al.* [1977] is described by a DT map that evolves in a closed hypercube of the real n-space and it is updated in a synchronous manner.

A neural network is said to be convergent, or completely stable, if each solution tends toward an equilibrium point (EP) [Hirsch, 1989; Cohen & Grossberg, 1983]. Convergence is one of the most fundamental properties of dynamical neural networks. Convergent neural networks are well suited to implement Content Addressable Memories (CAMs) and to solve combinatorial optimization problems and several other signal processing tasks in real time [Haykin, 1999; Zurada, 1992]. Especially, convergent CT-CNNs have proven effective for performing a variety of relevant image processing tasks in real time [Chua & Roska, 2005; Chua & Yang, 1988a]. Convergence of CT neural networks has been widely investigated using various techniques as Lyapunov method, the dichotomy of omega limit sets for cooperative neural networks, the global consistency of the decision scheme implemented by competitive neural networks and the Łojasiewicz inequality and the property of trajectories with finite length, see, e.g. [Cohen & Grossberg, 1983; Hirsch, 1989; Michel *et al.*, 1989; Yang *et al.*, 2018; Cheng *et al.*, 2006; Arik, 2020; Di Marco *et al.*, 2012b; Forti & Tesi, 2004] and references therein.

One classic result is that a CT-CNN is convergent if the interconnection matrix satisfies some symmetry condition [Chua & Yang, 1988b; Forti & Tesi, 2001]. Unfortunately, such a result cannot be directly applied to DT-CNNs and in fact the study of convergence of DT-CNNs is much more subtle than that of their CT counterparts. Indeed, even a simple first-order DT-CNN can exhibit persistent oscillations or a more complicated behavior. A similar situation holds for classes of nonsymmetric neural networks. For instance, cooperative CT-CNNs enjoy convergence under an irreducibility assumption of the interconnections as a consequence of the theory of monotone flows and the dichotomy of omega-limit sets [Hirsch, 1982; Di Marco *et al.*, 2010, 2011, 2012a], however, analogous results are not available for DT cooperative neural networks [Hirsch, 1989].

In this paper, we are mainly interested in studying the convergence of the DT-CNN model introduced in [Chen & Shih, 2004]. In that paper, it is shown that a DT-CNN is convergent if the cloning template generates an interconnection matrix T that is *symmetric and positive definite*, the DT-CNN has regular parameters, which implies that

there are isolated EPs, and an additional assumption is satisfied (see condition (H) in [Chen & Shih, 2004]). It is stressed that a large part of the symmetric cloning templates used in the applications to image processing tasks actually generate an interconnection matrix T that has both positive and negative eigenvalues, i.e. it is not positive definite (see Sec. 5 for more details). More generally, relevant techniques for associative memory design, as those based on a singular value decomposition [Michel *et al.*, 1991], yield indefinite symmetric interconnection matrices. Therefore, it would be of great interest in view of the applications of DT-CNNs to extend the convergence result in [Chen & Shih, 2004] in order to include symmetric interconnection matrices for which the positive definiteness assumption fails.

In this paper, it is shown that a DT-CNN is convergent when T is symmetric and, in the case where $T + E_n$ is not positive-semidefinite, where E_n is the $n \times n$ unit matrix, the step size of Euler's discretization scheme does not exceed a given bound (Theorem 1). Theorem 1 extends the quoted result in [Chen & Shih, 2004], since it can be applied to establish convergence for any symmetric interconnection matrix T, whether it is positive definite or not. Moreover, differently from that paper, we do not require additional assumptions as condition (H) in [Chen & Shih, 2004]. It is also shown that, as a consequence of the local and space-invariant interconnections: (1) the bound on the step size can be readily estimated on the basis of the elements of the feedback cloning template only; (2) the estimate turns out to be independent of the dimension of the DT-CNN array. These are two key properties in view of the application of large DT-CNN arrays to image processing tasks.

The main results in the paper are proved via a Lyapunov approach in combination with LaSalle's Invariance Principle for DT systems (Sec. 3.1). In particular, to prove that a given Lyapunov (energy) function is decreasing along the DT-CNN solutions, some fundamental properties and inequalities of the projection onto a closed convex set are used. The result in Theorem 1 is compared in the paper with convergence results for other different DT neural network models in the literature, as the Brain-State-in-a-Box model [Golden, 1986] (Sec. 3.3). Theorem 1 is illustrated with simulation examples including the application to typical templates for image processing (Sec. 5). Some basic examples are also specifically worked out to discuss tightness of the bound on the sampling interval in relation to convergence (Sec. 3.2).

2. Continuous-Time and Discrete-Time Cellular Neural Networks

A standard CNN [Chua & Yang, 1988b] is a special type of CT neural network characterized by *local* and *space-invariant* interconnections. More precisely, a CT-CNN is an aggregate of identical cells (or clones) on a regular array where only neighboring cells can interact directly with each other while distant cells can interact due to the propagation effects. The local and space-invariant interconnection structure is typically defined via a so-called *cloning template* that specifies the extent of the neighborhood of direct influence of each cell and the values of the interconnection strengths.

In this paper, we will consider 2D and 1D standard CNN arrays. A 2D $M \times N$ CT-CNN satisfies the system of differential equations

$$C_x \frac{dv_{xij}}{dt} = -\frac{1}{R_x} v_{xij} + \sum_{C(k,l) \in N_r(i,j)} A(i,j;k,l) v_{ykl} + \sum_{C(k,l) \in N_r(i,j)} B(i,j;k,l) v_{ukl} + K \quad (1)$$

for $1 \leq i \leq M$, $1 \leq j \leq N$, where C_x is the cell capacitor and R_x the cell resistance, moreover, for any positive integer r, $N_r(i,j) = \{C(k,l) : \max\{|k-i|, |l-j\} \leq r; 1 \leq k \leq M; 1 \leq l \leq N\}$, is the r-neighborhood of cell $C(i,j)$. Henceforth, for simplicity, we let $r = 1$. The quantities v_{xij}, v_{yij} and v_{uij} are the state, the output and the input of cell $C(i,j)$, respectively, whereas K is a bias. The terms $A(i,j;k,l)$ are the feedback interconnections of cell $C(i,j)$ with neighboring cells, while $B(i,j;k,l)$ are referred to as control inputs from neighboring cells to cell $C(i,j)$. The output of cell $C(i,j)$ is given by the typical three-segment piecewise-linear activation function $s(\cdot)$, i.e.

$$v_{yij} = s(v_{xij}) = \frac{1}{2}(|v_{xij} + 1| - |v_{xij} - 1|).$$

For a 2D CT-CNN array we assume in the paper that there are fixed (or Dirichlet) boundary conditions, i.e. $v_{xij} = 0$ if we have either $i \in \{0, M+1\}$ or $j \in \{0, N+1\}$.

It is useful to rewrite the equations using the notion of a cloning template. Since $r = 1$, consider the space-invariant feedback cloning template

$$\alpha = \begin{pmatrix} \alpha_{-1,-1} & \alpha_{-1,0} & \alpha_{-1,1} \\ \alpha_{0,-1} & \alpha_{0,0} & \alpha_{0,1} \\ \alpha_{1,-1} & \alpha_{1,0} & \alpha_{1,1} \end{pmatrix} \in \mathbb{R}^{3\times 3}$$

and input (control) cloning template

$$\beta = \begin{pmatrix} \beta_{-1,-1} & \beta_{-1,0} & \beta_{-1,1} \\ \beta_{0,-1} & \beta_{0,0} & \beta_{0,1} \\ \beta_{1,-1} & \beta_{1,0} & \beta_{1,1} \end{pmatrix} \in \mathbb{R}^{3\times 3}.$$

Then, in symbolic form the CT-CNN equations can be written as

$$\begin{aligned} C_x \frac{dv_{xij}}{dt} &= -\frac{1}{R_x} v_{xij} + \alpha \star v_{yij} + \beta \star v_{uij} + K \\ &= -\frac{1}{R_x} v_{xij} + \alpha_{-1,-1} v_{yi-1j-1} + \alpha_{-1,0} v_{yi-1j} \\ &\quad + \alpha_{-1,1} v_{yi-1j+1} + \alpha_{0,-1} v_{yij-1} + \alpha_{0,0} v_{yij} \\ &\quad + \alpha_{0,1} v_{yij+1} + \alpha_{1,-1} v_{yi+1j-1} + \alpha_{1,0} v_{yi+1j} \\ &\quad + \alpha_{1,1} v_{yi+1j+1} + \beta_{-1,-1} v_{ui-1j-1} \\ &\quad + \beta_{-1,0} v_{ui-1j} + \beta_{-1,1} v_{ui-1j+1} \\ &\quad + \beta_{0,-1} v_{uij-1} + \beta_{0,0} v_{uij} \\ &\quad + \beta_{0,1} v_{uij+1} + \beta_{1,-1} v_{ui+1j-1} \\ &\quad + \beta_{1,0} v_{ui+1j} + \beta_{1,1} v_{ui+1j+1} + K. \end{aligned} \tag{2}$$

The convolution operator $\star$ is explicitly defined in [Chua & Yang, 1988b, Definition 3].

A 2D CT-CNN is *symmetric* if we have $A(i, j; k, l) = A(k, l; i, j)$, $1 \le i, k \le M$, $1 \le j, l \le N$. This is equivalent to the feedback cloning template α that satisfies the conditions

$$\begin{aligned} \alpha_{-1,-1} = \alpha_{1,1}; \quad \alpha_{-1,0} = \alpha_{0,-1}; \\ \alpha_{-1,1} = \alpha_{1,-1}; \quad \alpha_{0,1} = \alpha_{1,0}. \end{aligned} \tag{3}$$

In the case of a 1D $M \times 1$ standard CT-CNN array the equations are

$$\begin{aligned} C_x \frac{dv_{xi}}{dt} &= -\frac{1}{R_x} v_{xi} + \sum_{C(j)\in N_r(i)} A(i, j) v_{yj} \\ &\quad + \sum_{C(j)\in N_r(i)} B(i, j) v_{uj} + K \end{aligned} \tag{4}$$

for $1 \le i \le M$, where $N_r(i) = C(j) : \max\{|j - i| \le r; 1 \le j \le M\}$. Once more, we assume $r = 1$. For 1D CT-CNNs we will consider three types of boundary conditions [Chua *et al.*, 1995]: periodic ($v_{x0} = v_{xM}$ and $v_{xM+1} = v_{x1}$), fixed (or Dirichlet — $v_{x0} = v_{xM+1} = 0$) and zero-flux (or reflective or Neumann — $v_{x0} = v_{x1}$ and $v_{xM+1} = v_{xM}$).

Consider the space-invariant feedback cloning template

$$\alpha = (\alpha_{-1} \quad \alpha_0 \quad \alpha_1) \in \mathbb{R}^{1\times 3}$$

and control cloning template

$$\beta = (\beta_{-1} \quad \beta_0 \quad \beta_1) \in \mathbb{R}^{1\times 3}.$$

Then, in symbolic form, the CT-CNN equations can be written as

$$\begin{aligned} C_x \frac{dv_{xi}}{dt} &= -\frac{1}{R_x} v_{xi} + \alpha \star v_{yj} + \beta \star v_{uj} + K \\ &= -\frac{1}{R_x} v_{xi} + \alpha_{-1} v_{yi-1} + \alpha_0 v_{yi} + \alpha_1 v_{yi+1} \\ &\quad + \beta_{-1} v_{ui-1} + \beta_0 v_{ui} + \beta_1 v_{ui+1} + K. \end{aligned} \tag{5}$$

For a 1D CT-CNN the symmetry condition $A(i, j) = A(j, i)$, $1 \le i \le M$, $1 \le j \le N$, is equivalent to the following condition for the feedback cloning template

$$\alpha_{-1} = \alpha_1. \tag{6}$$

In order to study convergence of CNNs, we find it useful to put the CNN equations in a more abstract vector form. By using a suitable ordering of rows or columns, a 2D CT-CNN can be described by the system of first-order differential equations

$$\dot{x} = -x + TS(x) + I, \tag{7}$$

where $n = M \times N$, $x \in \mathbb{R}^n$ is the vector of cells' capacitor voltages, $T = (T_{ij}) \in \mathbb{R}^{n\times n}$ is the interconnection matrix defined via the feedback cloning template and boundary conditions, $S(x) = (s(x_1), \ldots, s(x_n))^\top : \mathbb{R}^n \to \mathbb{R}^n$ is the vector of neuron activations and $I \in \mathbb{R}^n$ is the input defined by the control cloning template, the bias and the boundary conditions. For simplicity, we assumed that the cell capacitor and resistor have normalized values $C_x = 1$ F and $R_x = 1$ Ohm, respectively. Clearly, also a 1D CT-CNN array can be described by system (7) where $n = N$.

Let us choose a step size $\eta > 0$ and consider the samplings of the state variables $x_i(k) = x_i(k\eta)$

for $i = 1, 2, \ldots, n$ and $k = 0, 1, \ldots$ According to the forward Euler's rule, the discretization of the derivative $\dot{x}_i(t)$ at $t = k\eta$ is given by

$$\delta_i(x_i(k)) = \frac{x_i(k+1) - x_i(k)}{\eta}.$$

This yields the following synchronous difference scheme for (7)

$$\begin{aligned} x(k+1) &= F(x(k)) \\ &= x(k) + \eta(-x(k) + TS(x(k)) + I) \end{aligned} \quad (8)$$

for $k = 0, 1, \ldots$, where $F : \mathbb{R}^n \to \mathbb{R}^n$. Also, consider the cells' outputs $y(t) = S(x(t))$ and their samplings

$$y(k) = S(x(k)) \in H$$

for $k = 0, 1, \ldots$, where $H = [-1, 1]^n$ is the unit hypercube in $\mathbb{R}^n$. We have

$$y(k+1) = S(x(k) + \eta(-x(k) + TS(x_k) + I)) \quad (9)$$

for $k = 0, 1, \ldots$. Note that, while the states $x(k)$ evolve in $\mathbb{R}^n$, the outputs $y(k)$ are instead constrained to evolve into the closed hypercube H. We will refer henceforth to (8) (or (9)) as a standard DT-CNN.

An EP of the DT-CNN (8) is a point $\overline{x} \in \mathbb{R}^n$ such that $F(\overline{x}) = \overline{x}$. The corresponding output EP (OEP) is $\overline{y} = S(\overline{x})$.

Henceforth, as a standing assumption, we suppose that the step size satisfies

$$0 < \eta \leq 1.$$

This ensures that any solution $x(k)$, $k = 0, 1, \ldots$ of (8) is bounded. In fact, when $0 < \eta < 1$, [Chen & Shih, 2004, Proposition 2.1] implies that there exists a closed and bounded globally attracting set for (8). Moreover, in the special case $\eta = 1$ we obtain the map $x(k+1) = TS(x(k)) + I$, whose solutions are clearly bounded. Due to these properties, by applying Brouwer fixed point theorem it follows that there exists at least one EP of a DT-CNN. We denote by $\mathcal{E}$ the set of EPs.

3. Convergence of Discrete-Time Cellular Neural Networks

In Sec. 3.1, we provide the main results on convergence of DT-CNNs toward EPs. Then, in Sec. 3.2 we discuss the convergence results with some toy examples of low-dimensional DT-CNNs. Finally, Sec. 3.3 compares the obtained results with previous convergence results in the literature.

3.1. *Main results on convergence*

We recall the following [Hirsch, 1989].

Definition 3.1. The DT-CNN (8) is said to be convergent if each solution $x(k)$ tends to an EP as $k \to \infty$.

Suppose that $T = T^\top$ is symmetric, i.e. the feedback cloning template α satisfies either (3) for a 2D DT-CNN or (6) for a 1D DT-CNN. Consider for (8) the candidate Lyapunov function

$$W(x) = -\frac{1}{2}S^\top(x)(T - E_n)S(x) - S^\top(x)I,$$

where E_n denotes the $n \times n$ identity matrix. We remark that $W(\cdot)$ coincides with the Lyapunov function introduced by Chua and Yang to study symmetric CT-CNNs [Chua & Yang, 1988b]. Moreover, note that W is actually a function of the neuron output, i.e. $W(x) = W_y(y(x))$ where

$$W_y(y) = -\frac{1}{2}y^\top(T - E_n)y - y^\top I.$$

Since $T - E_n$ is symmetric, we have

$$\Gamma(y) \doteq \nabla W_y(y) = -(T - E_n)y - I.$$

With this notation, the DT-CNN (8) can be rewritten as

$$\begin{aligned} x(k+1) &= x(k) + \eta(-x(k) + y(k) \\ &\quad + (T - E_n)y(k) + I) \\ &= x(k) + \eta(y(k) - x(k)) - \eta\Gamma(y(k)). \end{aligned}$$

Let $\lambda_{\min}(\cdot)$ denote the minimum eigenvalue of a symmetric matrix. We consider the next hypotheses.

Assumption 1. The interconnection matrix T is symmetric and we have that either:

(1) $T + E_n$ is positive definite, i.e. $\lambda_{\min}(T + E_n) > 0$, or
(2) $T + E_n$ is positive semi-definite, i.e. $\lambda_{\min}(T + E_n) = 0$ and $\eta < 1$, or
(3) $T + E_n$ is not positive semi-definite, i.e. $\lambda_{\min}(T + E_n) < 0$ and

$$\eta < \eta_{\max} \doteq \frac{2}{|\lambda_{\min}(T - E_n)|} < 1. \quad (10)$$

Lemma 1. *Suppose that Assumption 1 holds. Then, there exists $\beta > 0$ such that*

$$\begin{aligned}\Delta W(k) &\doteq W(x(k+1)) - W(x(k)) \\ &\leq -\beta \|y(k+1) - y(k)\|^2 \leq 0\end{aligned}$$

for any $k = 0, 1, 2, \ldots$.

Proof. We have

$$\begin{aligned}&\Delta W(k) \\ &= -\frac{1}{2} y^\top(k+1)(T - E_n)y(k+1) - y^\top(k+1)I \\ &\quad + \frac{1}{2} y^\top(k)(T - E_n)y(k) + y^\top(k)I \\ &= -\frac{1}{2}(y(k) + \Delta y(k))^\top (T - E_n)(y(k) + \Delta y(k)) \\ &\quad - (y(k) + \Delta y(k))^\top I \\ &\quad + \frac{1}{2} y^\top(k)(T - E_n)y(k) + y^\top(k)I,\end{aligned}$$

where we denoted $\Delta y(k) = y(k+1) - y(k)$. Due to symmetry of $T - E_n$ we have

$$y(k)^\top (T - E_n)\Delta y(k) = \Delta^\top y(k)(T - E_n)y(k).$$

Then, a simple computation yields

$$\begin{aligned}\Delta W(k) &= -\Delta^\top y(k)(T - E_n)y(k) \\ &\quad - \frac{1}{2}\Delta^\top y(k)(T - E_n)\Delta y(k) - \Delta^\top y(k)I \\ &= \Delta^\top y(k)\Gamma(y(k)) \\ &\quad - \frac{1}{2}\Delta^\top y(k)(T - E_n)\Delta y(k).\end{aligned}$$

Now note that, given any point $x \in \mathbb{R}^n$, $y = S(x)$ is the projection of x onto the hypercube H, namely $y = S(x) = \arg\min_{z \in H} \|x - z\|$, where $\|\cdot\|$ is the 2-norm. Since H is convex, we have

$$\langle x - y, p - y \rangle \leq 0$$

for any $p \in H$, which is known as the Bourbaki–Cheney–Goldstein inequality or obtuse angle criterion [Ciarlet, 2013] ($\langle \cdot, \cdot \rangle$ denotes the scalar product). By applying this property with $x = x(k+1)$, $y = y(k+1) = S(x(k+1))$ and $p = y(k) \in H$, we obtain

$$\sigma \doteq \langle x(k+1) - y(k+1), y(k) - y(k+1) \rangle \leq 0.$$

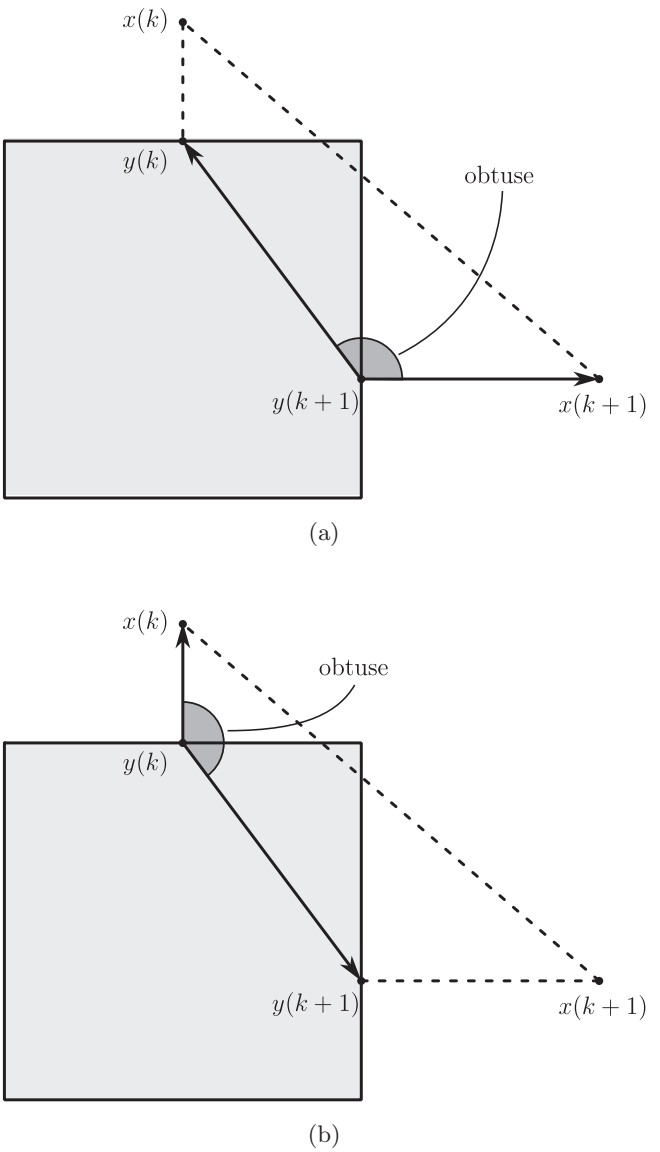

Fig. 1. Illustration of Bourbaki–Cheney–Goldstein inequality for a square $[-1, 1]^2$. By applying the inequality we obtain that: (a) The angle formed by vectors $x(k+1) - y(k+1)$ and $y(k) - y(k+1)$ is obtuse and (b) the same holds for the angle formed by vectors $y(k) - x(k)$ and $y(k+1) - y(k)$.

An illustration is given in Fig. 1(a) in a simple two-dimensional setting. Then, we have

$$\begin{aligned}\sigma &= \langle x(k+1) - y(k) + y(k) - y(k+1), \\ &\qquad y(k) - y(k+1) \rangle \\ &= \|\Delta y(k)\|^2 + \langle x(k+1) - y(k), y(k) - y(k+1) \rangle \\ &= \|\Delta y(k)\|^2 - \langle x(k+1) - y(k), \Delta y(k) \rangle \\ &= \|\Delta y(k)\|^2 - \langle x(k) + \eta(y(k) - x(k)) \\ &\qquad - \eta\Gamma(y(k)) - y(k), \Delta y(k) \rangle\end{aligned}$$

$$
\begin{aligned}
&= \|\Delta y(k)\|^2 \\
&\quad - \langle (1-\eta)(x(k)-y(k)) - \eta\Gamma(y(k)), \Delta y(k)\rangle \\
&= \|\Delta y(k)\|^2 - (1-\eta)\langle x(k)-y(k), \Delta y(k)\rangle \\
&\quad + \eta\langle \Gamma(y(k)), \Delta y(k)\rangle \le 0.
\end{aligned}
$$

By applying again the previous property of the convex set H with $x = x(k)$, $y = y(k) = S(x(k))$ and $p = y(k+1) \in H$ we obtain

$$
\begin{aligned}
&\langle x(k)-y(k), y(k+1)-y(k)\rangle \\
&\qquad = \langle x(k)-y(k), \Delta y(k)\rangle \le 0.
\end{aligned}
$$

An illustration of this property is given in Fig. 1(b). Hence, recalling also the standing assumption $0 < \eta \le 1$, we obtain

$$
\|\Delta y(k)\|^2 + \eta\langle \Gamma(y(k)), \Delta y(k)\rangle \le 0
$$

which yields

$$
\Delta^\top y(k)\Gamma(y(k)) \le -\frac{1}{\eta}\|\Delta y(k)\|^2.
$$

Therefore, we obtain

$$
\begin{aligned}
\Delta W(k) &\le -\frac{1}{\eta}\|\Delta y(k)\|^2 \\
&\quad - \frac{1}{2}\Delta^\top y(k)(T-E_n)\Delta y(k).
\end{aligned}
$$

Now note that

$$
\Delta^\top y(k)(T-E_n)\Delta y(k) \ge \lambda_{\min}(T-E_n)\|\Delta y(k)\|^2
$$

and then

$$
\begin{aligned}
\Delta W(k) &\le -\frac{1}{\eta}\|\Delta y(k)\|^2 - \frac{1}{2}\lambda_{\min}(T-E_n)\|\Delta y(k)\|^2 \\
&= -\left(\frac{1}{\eta} - \frac{1}{2} + \frac{1}{2}\lambda_{\min}(T)\right)\|\Delta y(k)\|^2.
\end{aligned}
$$

Consider case (1) where $\lambda_{\min}(T+E_n) > 0$. Since $0 < \eta \le 1$, we obtain

$$
\begin{aligned}
\Delta W(k) &\le -\left(1 - \frac{1}{2} + \frac{1}{2}\lambda_{\min}(T)\right)\|\Delta y(k)\|^2 \\
&= -\frac{1}{2}\lambda_{\min}(T+E_n)\|\Delta y(k)\|^2
\end{aligned}
$$

and the stated result holds with $\beta = (1/2)\lambda_{\min}(T+E_n) > 0$.

Then, consider case (2) where $\lambda_{\min}(T+E_n) = 0$. We have

$$
\begin{aligned}
\Delta W(k) &\le -\left(\frac{1}{\eta} - 1 + \frac{1}{2}\lambda_{\min}(T+E_n)\right)\|\Delta y(k)\|^2 \\
&= -\frac{1-\eta}{\eta}\|\Delta y(k)\|^2.
\end{aligned}
$$

The result follows with $\beta = (1-\eta)/\eta > 0$.

Finally, consider case (3), i.e. $\lambda_{\min}(T+E_n) < 0$ and so $\lambda_{\min}(T-E_n) < -2$. We obtain

$$
\begin{aligned}
\Delta W(k) &\le -\left(\frac{1}{\eta} + \frac{1}{2}\lambda_{\min}(T-E_n)\right)\|\Delta y(k)\|^2 \\
&= -\left(\frac{1}{\eta} - \frac{1}{2}|\lambda_{\min}(T-E_n)|\right)\|\Delta y(k)\|^2 \\
&= -\frac{|\lambda_{\min}(T-E_n)|}{2\eta} \\
&\quad \times \left(\frac{2}{|\lambda_{\min}(T-E_n)|} - \eta\right)\|\Delta y(k)\|^2.
\end{aligned}
$$

By taking into account (10), once more we have proved the stated result with

$$
\beta = \frac{|\lambda_{\min}(T-E_n)|}{2\eta}\left(\frac{2}{|\lambda_{\min}(T-E_n)|} - \eta\right) > 0.
$$

■

Assumption 2. Matrix $T - E_n$ and all of its principal submatrices are nonsingular.

This assumption implies that there exists a finite number of EPs for the DT-CNN and it corresponds to the hypothesis of regular parameters considered in [Chen & Shih, 2004].

Theorem 1. *If Assumptions 1 and 2 hold, then the DT-CNN (8) is convergent.*

Proof. Consider a solution $x(k)$ of (8) such that $x(0) = x_0 \in \mathbb{R}^n$. For $0 < \eta \le 1$, the solution is bounded and is contained for all large k in a compact attracting set $\Phi \subset \mathbb{R}^n$. Due to Lemma 1 and LaSalle's Invariance Principle for DT systems [Mei & Bullo, 2017], $W(k) \to c > -\infty$, while $x(k)$ tends to the largest invariant set contained in the set $\Upsilon = \{x \in \mathbb{R}^n : W(F(x)) = W(x)\}$, where F is as in (8). Recalling that $\beta > 0$, according to Lemma 1, we have $\Delta W(k) = 0$ if and only if $y(k+1) = y(k)$. Then, $x \in \Upsilon$ if and only if $S(F(x)) = S(x)$.

Following the in-depth analysis in [Chen & Shih, 2004], we can characterize the set Υ in the

following way. Let us decompose $\mathbb{R}^n$ in the usual way in 3^n subsets Λ_α indexed by $\alpha = (\alpha_1, \ldots, \alpha_n)^\top \in \mathbb{R}^n$ with $\alpha_i \in \{-1, 0, 1\}$, $i = 1, \ldots, n$, where $\Lambda_\alpha = \{x \in \mathbb{R}^n : -1 < x_i < 1, \alpha_i = 0; x_i \geq 1, \alpha_i = 1, x_i \leq -1, \alpha_i = -1\}$.

First, consider the linear region $\Lambda_{\alpha=0}$ and point

$$\xi_0 = (T - E_n)^{-1} I.$$

If $\xi_0 \in \Lambda_0$, then $\Upsilon_{\alpha=0} \doteq \Upsilon \cap \Lambda_0 = \{\xi_0\}$ and $S(\Upsilon_0) = \{\xi_0\}$. Otherwise, $\Upsilon_0 = \emptyset$.

Now, consider without loss of generality a partial saturation region defined by α such that $\alpha_i = 0$, $i = 1, \ldots, m$ and $\alpha_i \in \{-1, 1\}$, $i = m+1, \ldots, n$, for some $1 \leq m < n$. Let us consider the partitions

$$T = \begin{pmatrix} T^{LL} & T^{LS} \\ T^{SL} & T^{SS} \end{pmatrix}, \quad I = \begin{pmatrix} I^L \\ I^s \end{pmatrix},$$

where $T^{LL} \in \mathbb{R}^{m \times m}, T^{LS} \in \mathbb{R}^{m \times (n-m)}$, $T^{LS} \in \mathbb{R}^{(n-m) \times m}, T^{SS} \in \mathbb{R}^{(n-m) \times (n-m)}$, $I^L \in \mathbb{R}^L$, $I^S \in \mathbb{R}^{n-m}$ and the related partitions of the other vectors. Let

$$\xi^L = (T^{LL} - E_m)^{-1} (T^{LS} \alpha^S + I^L).$$

If $-1 < \xi_i^L < 1$, $i = 1, \ldots, m$, then

$$\Upsilon_\alpha \doteq \Upsilon \cap \Lambda_\alpha = \{x \in \Lambda_\alpha : S(x) = (\xi^L, \alpha^S)\}$$

and $S(\Upsilon_\alpha) = \{(\xi^L, \alpha^S)\}$. Otherwise, $\Upsilon_\alpha = \emptyset$.

Finally, consider a saturation region characterized by α such that $\alpha_i \in \{-1, 1\}$, $i = 1, \ldots, n$. In this case $\Upsilon_\alpha = \Upsilon \cap \Lambda_\alpha = \Lambda_\alpha$ and $S(\Lambda_\alpha) = \{\alpha\}$.

Summing up, Υ is contained in the union of at most 3^n disjoint subsets Υ_α of $\mathbb{R}^n$. Moreover, it can be readily verified that there is a minimum distance $\delta > 0$ between such sets. Namely, if we take any pair of sets $\Upsilon_{\overline{\alpha}}$ and $\Upsilon_{\hat{\alpha}}$ with $\overline{\alpha} \neq \hat{\alpha}$, then

$$\begin{aligned} d_y(\Upsilon_{\overline{\alpha}}, \Upsilon_{\hat{\alpha}}) &= \inf_{\overline{x} \in \Upsilon_{\overline{\alpha}}, \hat{x} \in \Upsilon_{\hat{\alpha}}} \|S(\overline{x}) - S(\hat{x})\| \\ &= \|S(\Upsilon_{\overline{\alpha}}) - S(\Upsilon_{\hat{\alpha}})\| \\ &\geq \delta > 0. \end{aligned}$$

As a simple illustrative example, consider a 2D DT-CNN with

$$T = \begin{pmatrix} 1.5 & 0.4 \\ 0.4 & 0.5 \end{pmatrix}; \quad I = \begin{pmatrix} 0.3 \\ 0 \end{pmatrix}.$$

The set Υ is the union of eight disjoint subsets $\Upsilon_{(-1,-1)}$, $\Upsilon_{(-1,1)}$, $\Upsilon_{(1,-1)}$, $\Upsilon_{(1,1)}$, $\Upsilon_{(-1,0)}$, $\Upsilon_{(1,0)}$, $\Upsilon_{(0,-1)}$ and $\Upsilon_{(0,0)}$, as shown in Fig. 2. The minimum distance between any pair of these subsets is found to be $\delta = 0.2 > 0$.

Let $\omega(x_0)$ be the omega-limit set of the considered solution, i.e. the set of points $z \in \mathbb{R}^n$ such that there exists a subsequence $h(k)$ such that $x(h(k)) \to z$ as $k \to \infty$. We have shown before that $\omega(x_0) \subset \Upsilon$. Now, we want to show that $\omega(x_0)$ is contained in only one of the previously identified subset Υ_α. To this end, we argue by contradiction assuming there are $\overline{\alpha} \neq \hat{\alpha}$ such that $\omega(x_0) \subset \Upsilon_{\overline{\alpha}} \cup \Upsilon_{\hat{\alpha}}$ and there exist $\overline{z} \in \omega(x_0) \cap \Upsilon_{\overline{\alpha}}$ and $\hat{z} \in \omega(x_0) \cap \Upsilon_{\hat{\alpha}}$. Hence, there are subsequences $h_1(k)$, $h_2(k)$ such that $x(h_1(k)) \to \overline{z}$ and $x(h_2(k)) \to \hat{z}$ as $k \to \infty$. Consider the sets $B_y(\Upsilon_{\overline{\alpha}}, \delta/4) = \{x \in \mathbb{R}^n : \|S(x) - S(\Upsilon_{\overline{\alpha}})\| < \delta/4\}$ and $B_y(\Upsilon_{\hat{\alpha}}, \delta/4) = \{x \in \mathbb{R}^n : \|S(x) - S(\Upsilon_{\hat{\alpha}})\| < \delta/4\}$. Consider the compact set

$$\Gamma \doteq \overline{\Phi \backslash \{B_y(\Upsilon_{\overline{\alpha}}) \cup B_y(\Upsilon_{\hat{\alpha}})\}},$$

where the overline denotes the closure. Clearly

$$\omega(x_0) \cap \Gamma = \emptyset. \tag{11}$$

From Lemma 1 we have that

$$\Delta W(k) \leq -\beta \|y(k+1) - y(k)\|^2$$

with $\beta > 0$. Since $W(x(k)) \to c > -\infty$, this implies that $\|y(k+1) - y(k)\| \to 0$ as $k \to \infty$. Hence, there exists $\overline{k}$ such that $\|y(k+1) - y(k)\| < \delta/4$ for $k \geq \overline{k}$. Since $\overline{z}, \hat{z} \in \omega(x_0)$, there exist $p(2) > p(1) \geq \overline{k}$ such that $x(p(1)) \in B_y(\overline{z}, \delta/4)$ and $x(p(2)) \in B_y(\hat{z}, \delta/4)$. However, since $\|y(k+1) - y(k)\| < \delta/4$ for any $k \geq \overline{k}$, it is seen that there exists $q(1)$ such that $p(2) > q(1) > p(1)$ and $x(q(1)) \in \Gamma$. This argument can be iterated so that we have shown that there exists a subsequence $q(k)$, with $q(k) \to \infty$ as $k \to \infty$, such that $x(q(k)) \in \Gamma$. Since Γ is compact, there exists $\tilde{z} \in \Gamma$, $\tilde{z} \neq \overline{z}, \hat{z}$ which is an accumulation point of $x(k)$, hence, $\tilde{z} \in \omega(x_0)$. However, this contradicts (11).

The previous argument shows that $\omega(x_0) \subset \Upsilon_\alpha$ for some α. Let $y_\alpha = S(\Upsilon_\alpha)$. Then, we have shown that $y(k) \to y_\alpha$ as $k \to \infty$. Let us define $x_\alpha = T y_\alpha + I$, $\Delta y(k) = y(k) - y_\alpha$ and $\Delta x(k) = x(k) - x_\alpha$. We want to prove that $\|\Delta x(k)\| \to 0$ as $k \to +\infty$, i.e. for any $\varepsilon > 0$ there exist $\overline{k}$ such that $\|\Delta x(k)\| \leq \varepsilon$ for any $k > \overline{k}$. We have $\|\Delta y(k)\| \leq 2\sqrt{n}$ for any k, and $\|\Delta y(k)\| \to 0$ as $k \to +\infty$, as a consequence, there exists $\tilde{k}$ such that $\|\Delta y(k)\| < \varepsilon/(4\|T\|)$ for any $k > \tilde{k}$, where $\|T\|$ is the induced 2-norm of T. Due to the Variation-of-Constants Formula applied

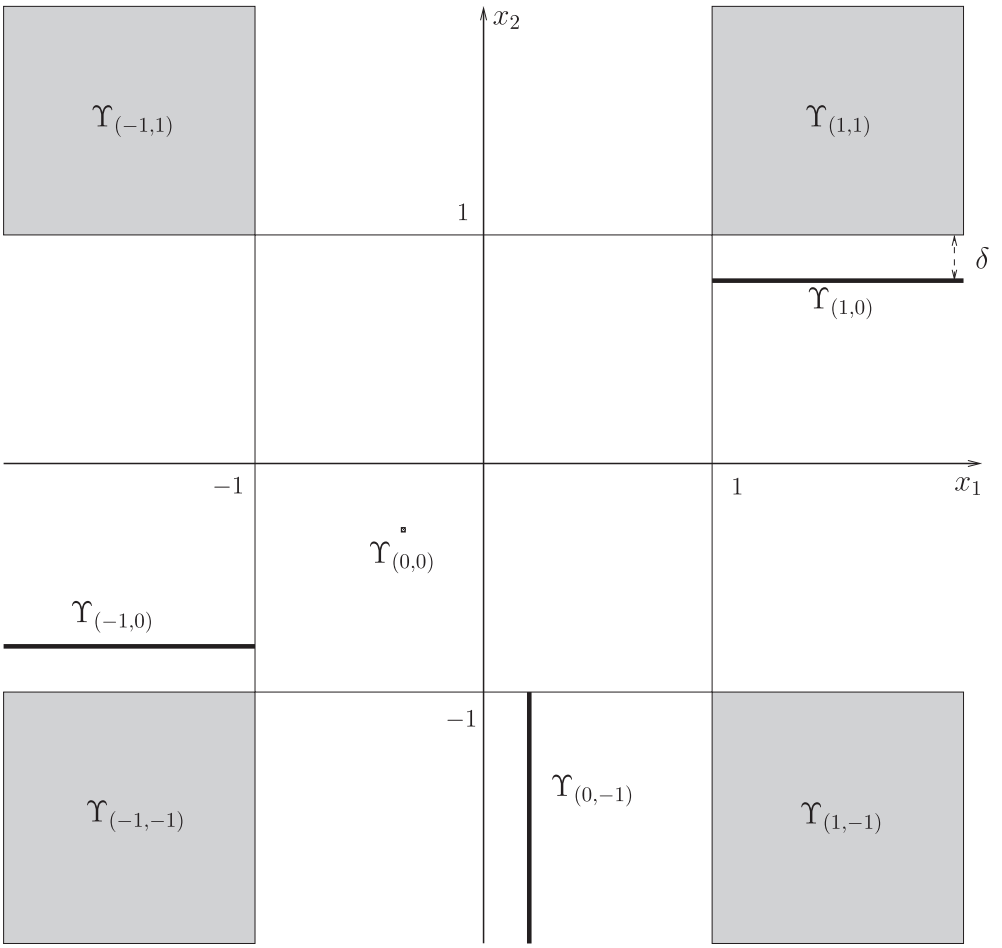

Fig. 2. Subsets Υ_α for a 2D DT-CNN. The minimum distance between any pair of these subsets is $\delta = 0.2$.

to (8), we obtain

$$x(k) = (1-\eta)^k x(0) + \sum_{i=1}^{k} (1-\eta)^{k-i} \eta (T y(i-1) + I)$$

and, after some manipulations,

$$\Delta x(k) = (1-\eta)^k x(0) + (T y_\alpha + I) \times \left(\eta \sum_{i=1}^{k} (1-\eta)^{k-i} - 1 \right) + \sum_{i=1}^{\tilde{k}} (1-\eta)^{k-i} \eta T \Delta y(i-1) + \sum_{i=\tilde{k}+1}^{k} (1-\eta)^{k-i} \eta T \Delta y(i-1).$$

Since $0 < \eta \leq 1$, we have

$$\eta \sum_{i=1}^{k} (1-\eta)^{k-i} - 1 = -(1-\eta)^k$$

$$\eta \sum_{i=1}^{\tilde{k}} (1-\eta)^{k-i} = (1-\eta)^{k-\tilde{k}} - (1-\eta)^k \leq (1-\eta)^{k-\tilde{k}}$$

$$\eta \sum_{i=\tilde{k}+1}^{k} (1-\eta)^{k-i} = 1 - (1-\eta)^{k-\tilde{k}} \leq 1$$

which implies

$$\|\Delta x(k)\| \leq |1-\eta|^k \|x(0)\| + (\|T\| \|y_\alpha\| + \|I\|) |1-\eta|^k + 2\sqrt{n} \|T\| |1-\eta|^{k-\tilde{k}} + \|T\| \frac{\varepsilon}{4\|T\|}.$$

Additionally, there exist k_1, k_2, k_3 such that

$$|1-\eta|^k \leq \frac{\varepsilon}{4\|x(0)\|}$$

for any $k > k_1$

$$|1-\eta|^k \leq \frac{\varepsilon}{4(\|T\|\|y_\alpha\| + \|I\|)}$$

for any $k > k_2$ and

$$|1-\eta|^{k-\tilde{k}} \leq \frac{\varepsilon}{8\sqrt{n}\|T\|}$$

for any $k > k_3$. By picking $\overline{k} = \max\{k_1, k_2, k_3\}$ we have that, for any $k > \overline{k}$

$$\|\Delta x(k)\| \leq \frac{\varepsilon}{4} + \frac{\varepsilon}{4} + \frac{\varepsilon}{4} + \frac{\varepsilon}{4} = \varepsilon$$

thus proving that $\|\Delta x(k)\| \to 0$ when $k \to +\infty$. Then, $x(k) \to x_\alpha = Ty_\alpha + I$ when $k \to +\infty$, where x_α is an EP and y_α is the corresponding OEP of the DT-CNN. ■

3.2. *Basic examples on convergence*

We provide a number of low-dimensional toy examples to discuss the result on convergence of DT-CNNs in Theorem 1. In particular, we focus on the tightness of bound for convergence $\eta_{\max}$ in (10). In Sec. 5, we will then apply the convergence results to some relevant classes of DT-CNNs defined by cloning templates used for image processing tasks.

Example 3.1. Consider the three-cell DT-CNN with interconnection matrix

$$T = \begin{pmatrix} 0.14 & 0.93 & -1.13 \\ 0.93 & -0.62 & -0.61 \\ -1.13 & -0.61 & -0.72 \end{pmatrix}$$

and input $I = (-0.1, -0.1, -0.1)^\top$. We have $\lambda_{\min}(T + E_3) = -0.5$, i.e. $T + E_3$ is not positive-semidefinite. Moreover, $\eta_{\max} = 0.8$. Suppose we choose $\eta = 0.99 > \eta_{\max}$ and let $(x_1(0), x_2(0), x_3(0)) = (0.58, -1.28, -0.54)$. Figure 3 shows the evolution of the states $x_i(k)$ and outputs $y_i(k)$, $i = 1, 2, 3$ and $k = 0, 1, \ldots, 150$, while Fig. 4 depicts the evolution of the energy $W(x(k))$, $k = 0, 1, \ldots, 150$. The example clarifies that when the bound (10) is violated, the behavior of the energy can be non-monotone and moreover the solutions display large nonvanishing oscillations.

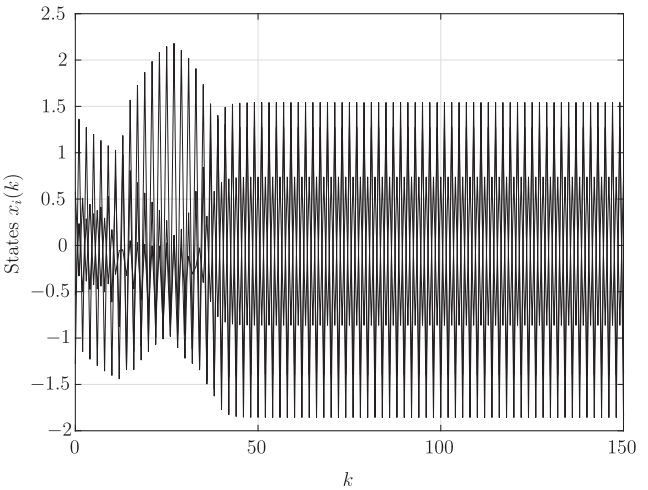

(a)

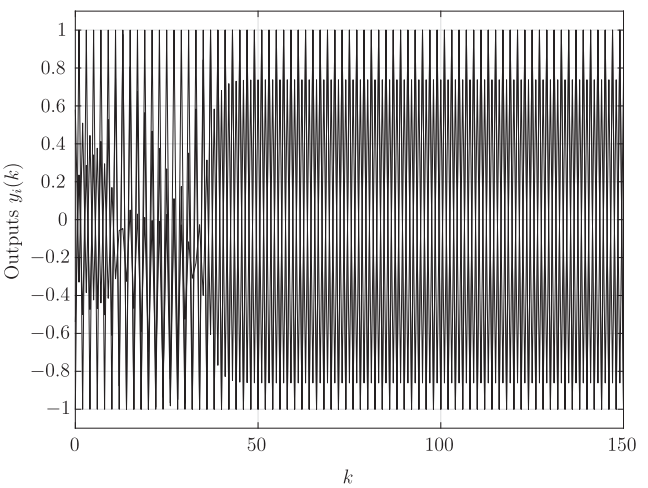

(b)

Fig. 3. (a) States and (b) outputs of DT-CNN in Example 3.1.

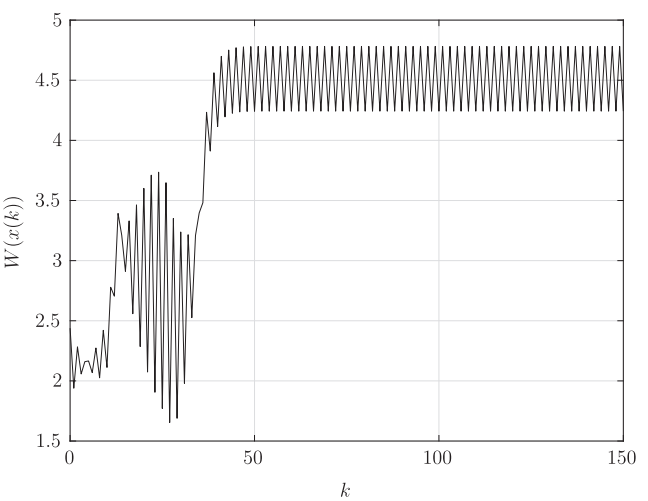

Fig. 4. Behavior of the energy of DT-CNN in Example 3.1.

Example 3.2. Consider the three-cell DT-CNN with interconnection matrix

$$T = \begin{pmatrix} -0.57 & -0.78 & 0.56 \\ -0.78 & -0.22 & 2.00 \\ 0.56 & 2.00 & 0.19 \end{pmatrix}$$

and input $I = (-0.1, -0.1, -0.1)^\top$. We have $\lambda_{\min}(T + E_3) = -1.498$ and $\eta_{\max} = 0.572$. Suppose we choose $\eta = 0.98 > \eta_{\max}$ and let $(x_1(0), x_2(0), x_3(0)) = (-0.43, -0.19, -0.54)$. Figure 5 displays the evolution of the states and outputs, while Fig. 6 shows the evolution of the energy. It is seen that, although η quite largely exceeds the bound $\eta_{\max}$, yet the energy decreases and moreover the state variables tend to constant values. This means that (10) is in general a sufficient, but not a necessary condition, for energy minimization and convergence of solutions.

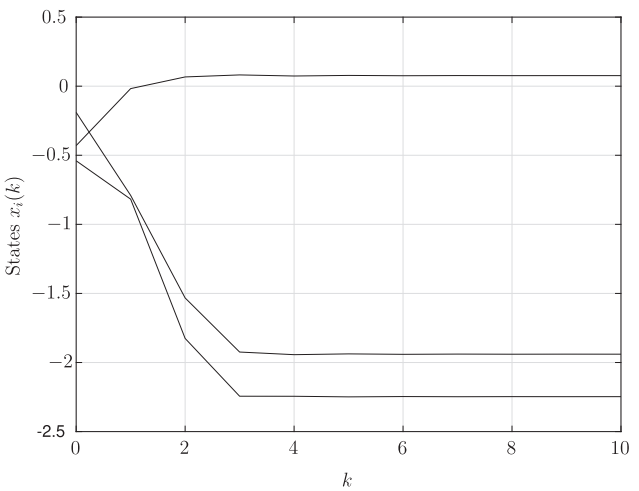

(a)

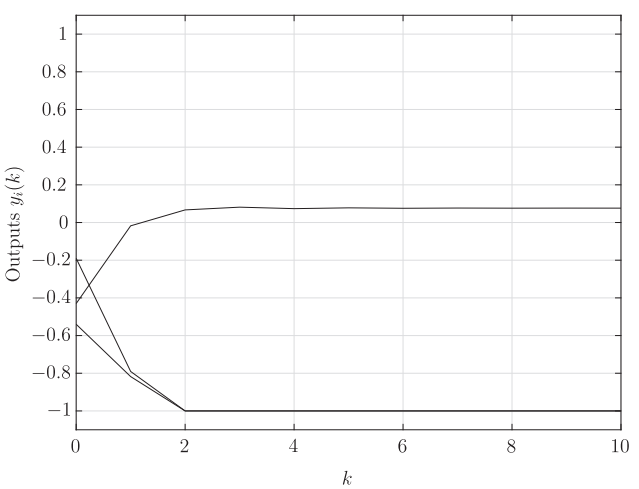

(b)

Fig. 5. (a) States and (b) outputs of DT-CNN in Example 3.2.

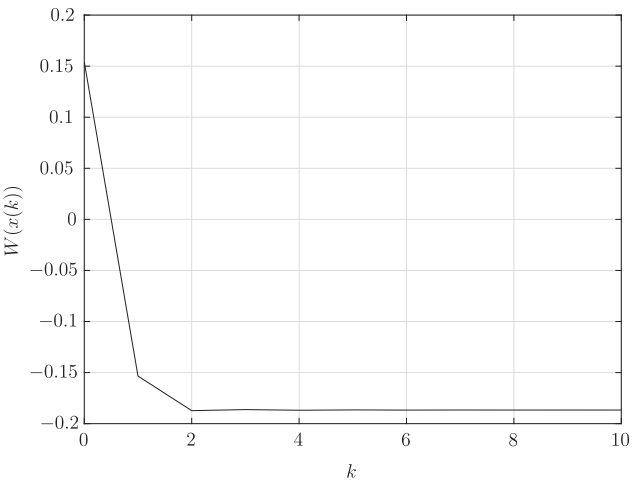

Fig. 6. Behavior of the energy of DT-CNN in Example 3.2.

Example 3.3. Consider the three-cell DT-CNN with interconnection matrix

$$T = \begin{pmatrix} -2.3 & -0.9 & 0.2 \\ -0.9 & -0.7 & 0.8 \\ 0.2 & 0.8 & -2.0 \end{pmatrix}$$

and input $I = (-0.1, -0.1, -0.1)^\top$. We have $\lambda_{\min}(T + E_3) = -2.01$ and so $\eta_{\max} = 0.499$. First, suppose we choose $\eta = 0.49 < \eta_{\max}$ and let $(x_1(0), x_2(0), x_3(0)) = (1.1, -1.4, 0.3)$. Figure 7 shows the evolution of the states and outputs, while Fig. 8 displays the evolution of the energy. It is seen that, as predicted by Theorem 1, the energy decreases and the solution converges. Then, suppose that $\eta = 0.505 > \eta_{\max}$. The evolution of the states and outputs and the energy is depicted in Figs. 9 and 10, respectively, for the solution with the same initial condition. Note that, although η slightly exceeds the bound $\eta_{\max}$, yet the energy is no longer monotonically decreasing, moreover the state variables display nonvanishing oscillations. This shows that, for this DT-CNN, the bound (10) is a tight one for ensuring minimization of the energy and convergence.

Example 3.4. Consider the three-cell DT-CNN with interconnection matrix

$$T = \begin{pmatrix} 0.14 & 0.93 & -1.13 \\ 0.93 & -0.62 & -0.61 \\ -1.13 & -0.61 & -0.72 \end{pmatrix}$$

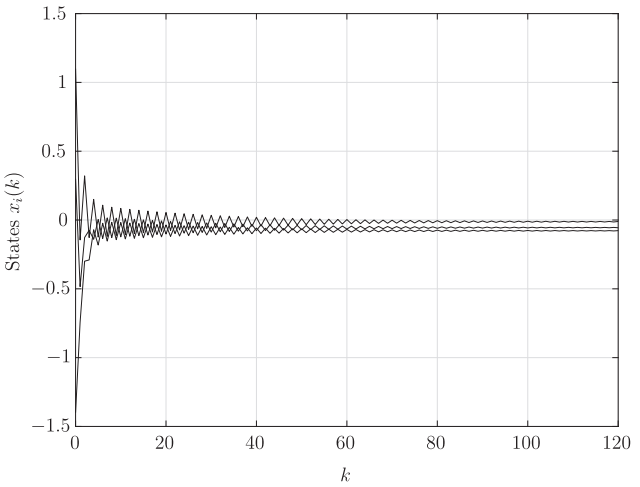

(a)

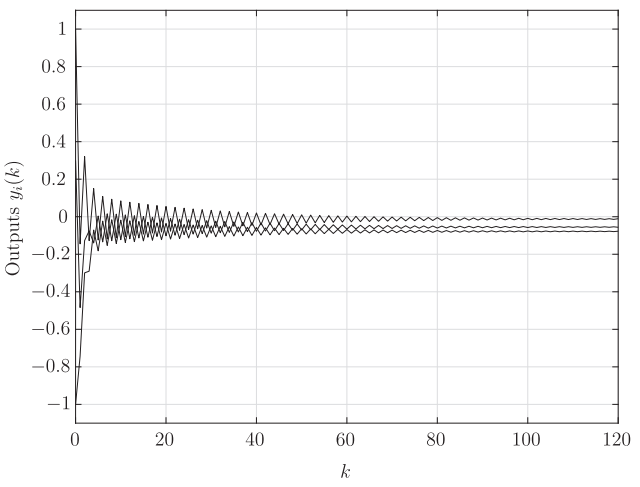

(b)

Fig. 7. (a) States and (b) outputs of DT-CNN in Example 3.3, case $\eta = 0.49$.

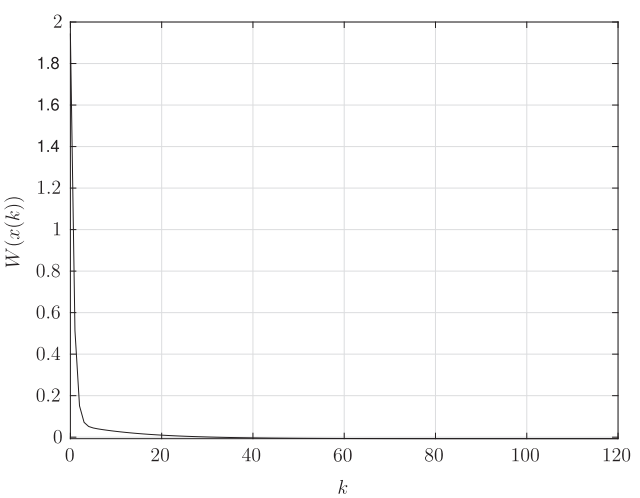

Fig. 8. Behavior of the energy of DT-CNN in Example 3.3, case $\eta = 0.49$.

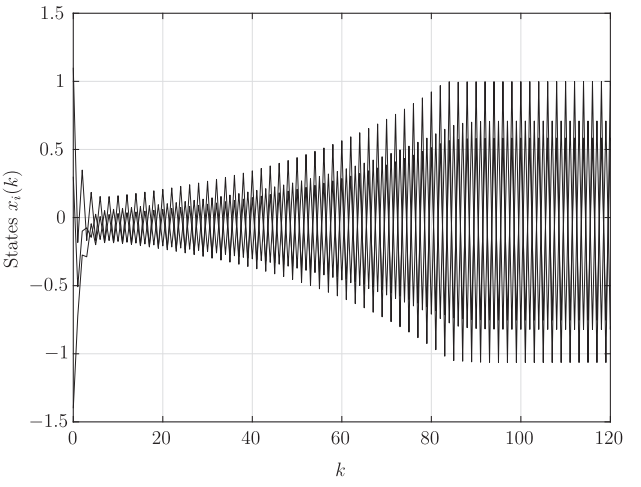

(a)

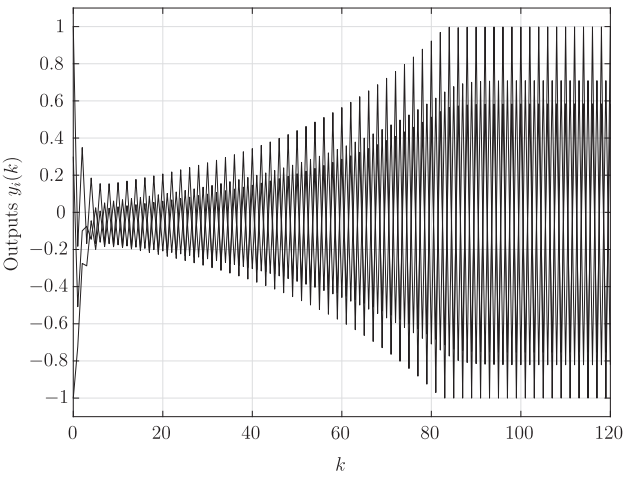

(b)

Fig. 9. (a) States and (b) outputs of DT-CNN in Example 3.3, case $\eta = 0.505$.

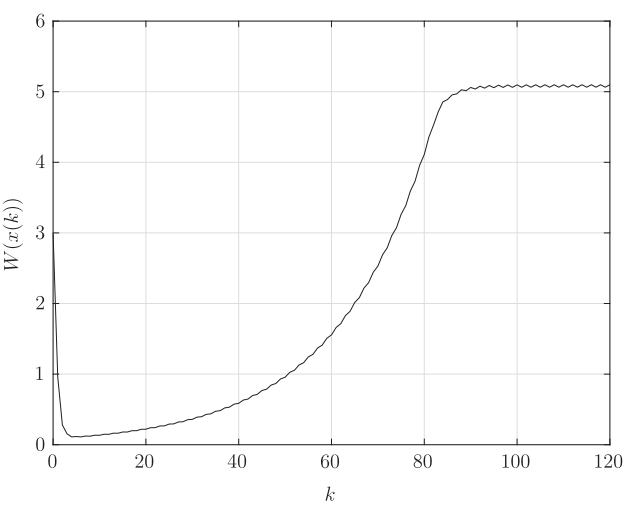

Fig. 10. Behavior of the energy of DT-CNN in Example 3.3, case $\eta = 0.505$.

and input $I = 0$. We have $\lambda_{\min}(T + E_3) = -0.5$ and so $\eta_{\max} = 0.8$. Suppose we choose $\eta = 0.99 > \eta_{\max}$ and let $(x_1(0), x_2(0), x_3(0)) = (1.82, -1.06, 1.68)$. Figure 11 displays the evolution of the states and outputs, while Fig. 12 shows the evolution of the energy $W(x(k))$. From simulations, the energy appears to be monotonically decreasing along the considered solution. This notwithstanding, the solution displays large nonvanishing oscillations. More precisely, it is seen that $x(k)$ tends to a cycle with period two, i.e. it oscillates between two distinct points $(1.7, 1.33, -0.81)$ and $(-1.7, -1.33, 0.81)$ that are not EPs of the DT-CNN but are characterized by the same value of the energy $W = 4.513$.

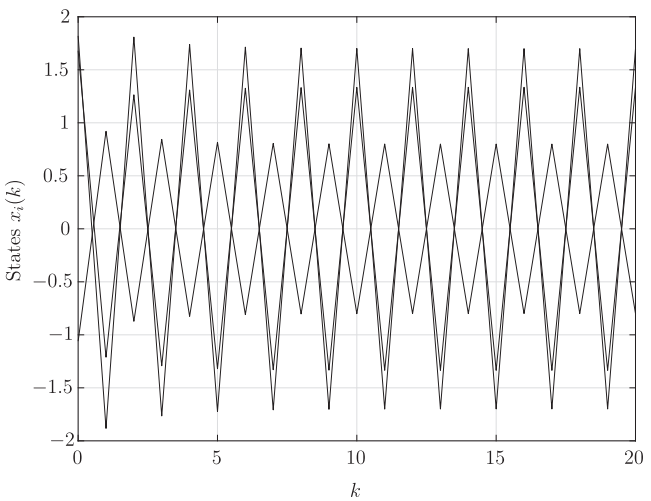

(a)

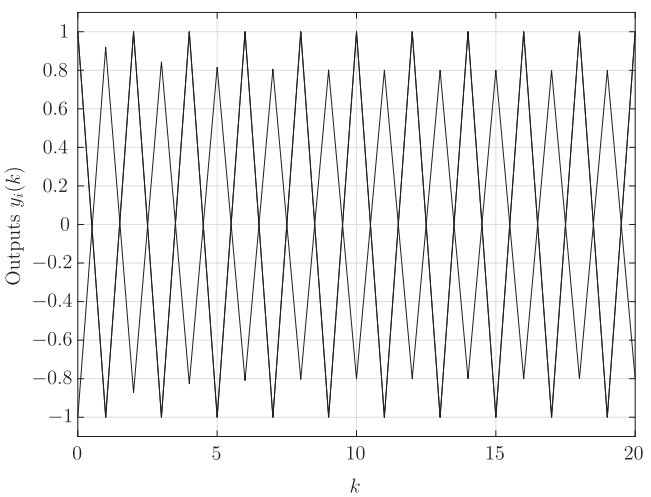

(b)

Fig. 11. (a) States and (b) outputs of DT-CNN in Example 3.4.

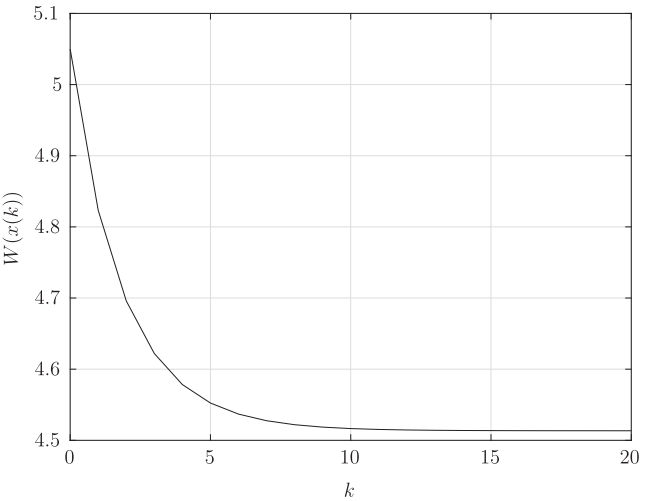

Fig. 12. Behavior of the energy of DT-CNN in Example 3.4.

3.3. *Discussion*

3.3.1. *Comparison with BSB*

In [Golden, 1986], the author considered the BSB model

$$X(k+1) = F_{\text{BSB}}(X(k)) = S(X(k) + \eta A X(k)), \tag{12}$$

where $X(k) \in \mathbb{R}^n$, $k = 1, 2, \ldots$, $A \in \mathbb{R}^{n \times n}$, $\eta > 0$ and $F_{\text{BSB}} : \mathbb{R}^n \to \mathbb{R}^n$. System (12) defining a BSB has some similarities with that defining the DT-CNN. Note that both the state $X(k)$ of a BSB and the output $y(k)$ of a DT-CNN evolve in H. However, while the state $X(k)$ of a BSB evolves in H, the state $x(k)$ of a DT-CNN instead evolves in the whole $\mathbb{R}^n$ space.

In the quoted paper Golden proved that the BSB minimizes the energy function

$$E(X) = -\frac{1}{2} X^\top A X$$

and any solution converges towards the set of EPs if $A = A^\top$ is symmetric and A is positive semidefinite or otherwise the step size satisfies the constraint $0 < \eta < 2/|\lambda_{\min}(A)|$. The result in Theorem 1 can be thought of as an extension to DT-CNN of the result by Golden. One difference is that for the DT-CNN we need the additional constraint $\eta \leq 1$ in order to guarantee that the state of the DT-CNN is bounded. This is instead not needed for BSB since in that case the state belongs to H and it is hence bounded by construction.

To better understand the significance of the results in this paper, it is worth to stress that,

although there are similarities between the BSB and DT-CNN models, yet their behavior may be quite different, as illustrated in the next example.

Example 3.5. Consider a two-neuron BSB with

$$A = \begin{pmatrix} 3 & 6 \\ 6 & -3 \end{pmatrix}.$$

In the interior of H the vector field defining the BSB is the linear vector field $F_{\mathrm{BSB}}(x) = x + \eta Ax$. If we choose

$$T = A + E_2 = \begin{pmatrix} 4 & 6 \\ 6 & -2 \end{pmatrix}$$

then the vector field F defining the DT-CNN coincides with that defining the BSB in the interior of H, i.e. $F = F_{\mathrm{BSB}}$. We consider such a DT-CNN as the DT-CNN corresponding to the BSB.

We have $\lambda_{\min}(T + E_2) = -4.7$, i.e. $T + E_2$ is not positive semi-definite and $\eta_{\max} = 2/|\lambda_{\min}(A)| = 2/|\lambda_{\min}(T - E_2)| = 0.298$. Let us choose for the BSB and the DT-CNN $\eta = 0.45$ and the same initial conditions $X(0) = x(0) = (0.5, -0.8)$. Figure 13 depicts the solution of the BSB, while Fig. 14 reports that of the DT-CNN. It is seen that, while the solution of the DT-CNN converges, the solution of the BSB has a remarkably different behavior, since it displays large nonvanishing oscillations.

The previous discussion shows that the similarities between the BSB and the DT-CNN models are only superficial. This justifies the analysis of DT-CNNs provided in this paper. It is worth to remark that analogous considerations hold also

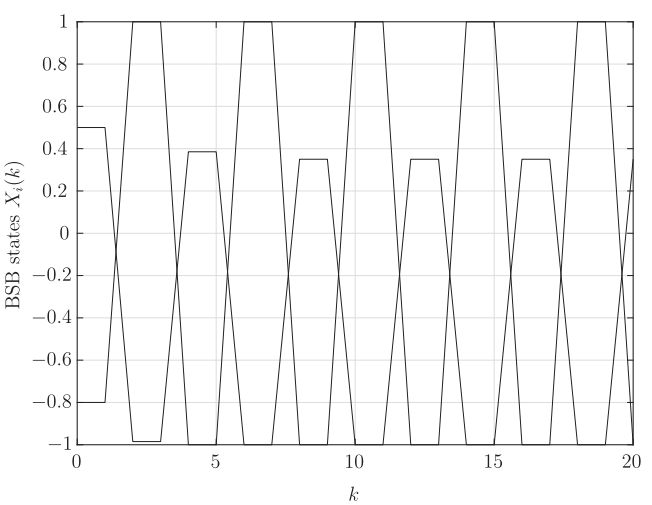

Fig. 13. States of BSB in Example 3.5.

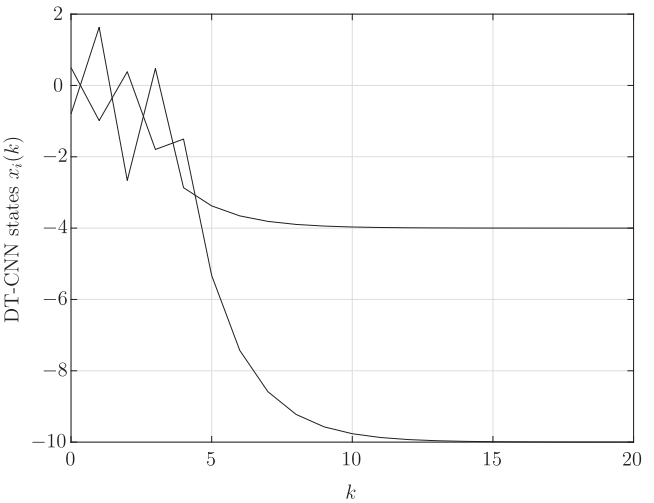

Fig. 14. States of DT-CNN in Example 3.5.

when comparing the dynamics of a CT-CNN with that of the full-range model of a CNN [Espejo *et al.*, 1996]. While the state of a CNN evolves in the whole $\mathbb{R}^n$ space, that of a full-range CNN is constrained to evolve in H. It is proved by Corinto and Gilli [2003] that a CNN and a full-range CNN in general display a different global dynamical behavior. For instance, while a CNN has convergent solutions, the corresponding full-range CNN displays a heteroclinic cycle with nonvanishing oscillations.

Finally, we remark that the technique used here to show that the energy of a DT-CNN is decreasing differs from that used by Golden. In particular, at the core of our proof are basic properties of the projection of a point onto a convex set (see the proof of Lemma 1).

3.3.2. *Other convergence results for DT-CNNs*

Chen and Shih [2004] proved that each solution of a DT-CNN (8) converges toward an EP if the DT-CNN interconnection matrix T is symmetric and positive definite, the DT-CNN has regular parameters (see [Chen & Shih, 2004, p. 2670]), and an additional technical assumption is satisfied. In particular, for regular parameters a DT-CNN has isolated EPs. Theorem 1 is an extension of the convergence result for symmetric DT-CNNs in [Chen & Shih, 2004] since it can be applied to establish convergence for any interconnection matrix T. In particular, a basic difference is that we do not require that T is positive definite. Regarding this point, we stress that a large part of the relevant symmetric

CNN templates used in the applications actually yield a matrix T which is not positive definite (cf. Sec. 5). Finally, it is noted once more that to prove Theorem 1 we used a different technique to evaluate the energy decrease, with respect to [Chen & Shih, 2004], based on the properties of the projection on a convex set.

4. Convergence of DT-CNNs Feedback Templates

In this section, we discuss the application of Theorem 1 to 2D and 1D CNN arrays. We assume that we are in the interesting case where T is symmetric but $T + E_n$ is not positive semidefinite, i.e. $\lambda_{\min}(T + E_n) < 0$, and so $\lambda_{\min}(T - E_n) < -2$, since in the other cases it is enough for the step size to choose $\eta \leq 1$ or $\eta < 1$ (Theorem 1). To apply Theorem 1 we need to evaluate the upper bound $\eta_{\max}$ in (10) for the step size, or, equivalently, the smallest eigenvalue $\lambda_{\min}(T - E_n)$. Recall that T is defined by the feedback cloning template and the boundary conditions. We stress that, in view of the applications to image processing tasks, we need estimates of these quantities that are applicable to large dimension DT-CNN arrays. Our goal is to demonstrate that, due to the local and space-invariant interconnection structure of a CNN, it is indeed possible to effectively evaluate $\eta_{\max}$ and $\lambda_{\min}(T - E_n)$. Moreover, the two estimates can be expressed through the elements of the feedback cloning template and they turn out to be independent of the dimension n of the CNN array.

4.1. *2D DT-CNNs*

It can be seen that for a symmetric 2D DT-CNN, T is a symmetric block Toeplix matrix. To the authors knowledge, no simple formula is available in general for the eigenvalues of $T - E_n$. With the next result we will evaluate $\eta_{\max}$ by providing an approximate estimate of $\lambda_{\min}(T - E_n)$ with a technique analogous to that used to prove Gershgorin-type results for localization of eigenvalues [Johnson *et al.*, 1993].

Theorem 2. *Consider a symmetric 2D DT-CNN. Then, we have*

$$\frac{2}{|\Theta_{2D}|} \leq \eta_{\max} \tag{13}$$

where we have let

$$\Theta_{2D} = -1 + \alpha_{0,0} - |\alpha_{-1,-1}| - |\alpha_{-1,0}| - |\alpha_{-1,1}| - |\alpha_{0,-1}| - |\alpha_{0,1}| - |\alpha_{1,-1}| - |\alpha_{1,0}| - |\alpha_{1,1}|.$$

Proof. Let $\nu \in \mathbb{R}^n$ be a (real) eigenvector corresponding to $\lambda_{\min}(T - E_n)$. Choose $i \in \{1, \ldots, n\}$ such that $|\nu_i| \geq |\nu_j|$ for all $j \in \{1, \ldots, n\}$. The relation $\lambda_{\min}(T - E_n)\nu = (T - E_n)\nu$ implies

$$|(\lambda_{\min}(T - E_n) - T_{ii} + 1)\nu_i| = \left|\sum_{j \neq i} T_{ij}\nu_j\right|$$

and, consequently

$$|\lambda_{\min}(T - E_n) - T_{ii} + 1| \leq \sum_{j \neq i} |T_{ij}| \frac{|\nu_j|}{|\nu_i|} \leq \sum_{j \neq i} |T_{ij}|$$

that is

$$T_{ii} - 1 - \sum_{j \neq i} |T_{ij}| \leq \lambda_{\min}(T - E_n) \leq T_{ii} - 1 + \sum_{j \neq i} |T_{ij}|. \tag{14}$$

Now, taking into account (2), we have $T_{ii} = \alpha_{0,0}$, while each line of T has at most eight non-null off-diagonal entries, namely the elements of the cloning template α different from $\alpha_{0,0}$. Then, we have

$$\begin{aligned}\lambda_{\min}(T - E_n) &\geq -1 + \alpha_{0,0} - |\alpha_{-1,-1}| - |\alpha_{-1,0}| - |\alpha_{-1,1}| \\ &\quad - |\alpha_{0,-1}| - |\alpha_{0,1}| - |\alpha_{1,-1}| \\ &\quad - |\alpha_{1,0}| - |\alpha_{1,1}| \\ &= \Theta_{2D}. \end{aligned} \tag{15}$$

Finally, note that since $T + E_n$ is not positive semidefinite, we have $\Theta_{2D} \leq \lambda_{\min}(T - E_n) < -2$ and so $2/|\Theta_{2D}| < 1$. ■

4.2. *1D DT-CNNs*

Consider a 1D symmetric DT-CNN. Let the feedback cloning template be $\alpha = (\alpha_1 \quad \alpha_0 \quad \alpha_1)$. Next we consider separately three different types of boundary conditions.

4.2.1. *Periodic boundary conditions*

In this case, we obtain a symmetric circulant interconnection matrix

$$T = \begin{pmatrix} \alpha_0 & \alpha_1 & 0 & 0 & \cdots & \alpha_1 \\ \alpha_1 & \alpha_0 & \alpha_1 & 0 & \cdots & 0 \\ 0 & \alpha_1 & \alpha_0 & \alpha_1 & \cdots & 0 \\ \vdots & \ddots & \ddots & \ddots & \ddots & \vdots \\ 0 & \cdots & 0 & \alpha_1 & \alpha_0 & \alpha_1 \\ \alpha_1 & \cdots & 0 & 0 & \alpha_1 & \alpha_0 \end{pmatrix}.$$

The eigenvalues of T are explicitly given as [Davis, 2012]

$$\lambda_i = \alpha_0 + 2\alpha_1 \cos\left(\frac{2\pi i}{n}\right)$$

with $i = 0, 1, \ldots, n-1$. Therefore we have

$$\lambda_{\min}(T - E_n) = \alpha_0 - 1 - 2|\alpha_1|$$

if n is even, while

$$\lambda_{\min}(T - E_n) = \alpha_0 - 1 + 2\alpha_1 \cos\left(\frac{\pi(n-1)}{n}\right)$$

if n is odd and $\alpha_1 \geq 0$, or

$$\lambda_{\min}(T - E_n) = \alpha_0 - 1 - 2|\alpha_1|$$

if n is odd and $\alpha_1 < 0$.

These facts yield the following result.

Theorem 3. *Consider a symmetric 1D DT-CNN and periodic boundary conditions. Then*:

(1)

$$\eta_{\max} = \frac{2}{|\alpha_0 - 1 - 2|\alpha_1||} \tag{16}$$

if n is even or, otherwise, if n is odd and $\alpha_1 < 0$;

(2)

$$\eta_{\max} = \frac{2}{\left|\alpha_0 - 1 + 2\alpha_1 \cos\left(\frac{\pi(n-1)}{n}\right)\right|} \tag{17}$$

if n is odd and $\alpha_1 \geq 0$.

4.2.2. *Fixed boundary conditions*

In this case, we obtain a symmetric tridiagonal Toeplitz interconnection matrix

$$T = \begin{pmatrix} \alpha_0 & \alpha_1 & 0 & 0 & \cdots & 0 \\ \alpha_1 & \alpha_0 & \alpha_1 & 0 & \cdots & 0 \\ 0 & \alpha_1 & \alpha_0 & \alpha_1 & \ddots & 0 \\ \vdots & \ddots & \ddots & \ddots & \ddots & \vdots \\ 0 & \cdots & 0 & \alpha_1 & \alpha_0 & \alpha_1 \\ 0 & \cdots & 0 & 0 & \alpha_1 & \alpha_0 \end{pmatrix}.$$

The eigenvalues of T are explicitly given as [Davis, 2012]

$$\lambda_i = \alpha_0 + 2|\alpha_1| \cos\left(\frac{\pi i}{n+1}\right)$$

with $i = 1, \ldots, n$. Then, we have

$$\lambda_{\min}(T - E_n) = \alpha_0 - 1 + 2|\alpha_1| \cos\left(\frac{\pi n}{n+1}\right).$$

Therefore, we obtain the next result.

Theorem 4. *Consider a symmetric 1D DT-CNN with fixed boundary conditions. Then*:

$$\eta_{\max} = \frac{2}{\left|\alpha_0 - 1 + 2|\alpha_1| \cos\left(\frac{\pi n}{n+1}\right)\right|}. \tag{18}$$

4.2.3. *Zero-flux boundary conditions*

In this case, we obtain the following interconnection matrix

$$T = \begin{pmatrix} \alpha_0 + \alpha_1 & \alpha_1 & 0 & 0 & \cdots & 0 \\ \alpha_1 & \alpha_0 & \alpha_1 & 0 & \cdots & 0 \\ 0 & \alpha_1 & \alpha_0 & \alpha_1 & \ddots & 0 \\ \vdots & \ddots & \ddots & \ddots & \ddots & \vdots \\ 0 & \cdots & 0 & \alpha_1 & \alpha_0 & \alpha_1 \\ 0 & \cdots & 0 & 0 & \alpha_1 & \alpha_0 + \alpha_1 \end{pmatrix}.$$

To the authors' knowledge, there is no readily available formula for the eigenvalues of such a matrix. However, we can resort again to a Gershgorin-type

technique, and obtain the following (details of the proof are omitted).

Theorem 5. *Let us consider a symmetric 1D DT-CNN with zero-flux boundary conditions. Then, we have*

$$\frac{2}{|\Theta_{1D}|} \leq \eta_{\max} \tag{19}$$

where we have let

$$\Theta_{1D} = \alpha_0 - 1 - 2|\alpha_1|. \tag{20}$$

4.3. *Remarks*

(1) In the case of 1D DT-CNNs with periodic or fixed boundary conditions we obtained an exact estimate of $\lambda_{\min}(T - E_n)$ and the bound $\eta_{\max}$ in Theorem 1, while for 2D DT-CNNs and 1D DT-CNNs with zero-flux boundary conditions we obtained approximate estimates of the same quantities.

(2) It can be shown that for all considered classes of 1D DT-CNNs we have

$$\alpha_0 - 1 - 2|\alpha_1| \leq \lambda_{\min}(T - E_n) \tag{21}$$

and then

$$\frac{2}{|\alpha_0 - 1 - 2|\alpha_1||} \leq \eta_{\max}.$$

This implies that for both 2D and 1D DT-CNNs we have at our disposal simple forms of all the estimates of $\eta_{\max}$ which depend only upon the elements of the feedback cloning template α and are independent of the dimension n of the array.

(3) All the techniques here discussed for finding the estimates can be immediately extended to 2D or 1D DT-CNNs with $r > 1$ as those studied for instance in [Thiran *et al.*, 1995].

5. Simulation of Relevant Classes of DT-CNNs Templates

5.1. *2D DT-CNNs*

In this section, we will discuss a number of applications of 2D DT-CNNs to image processing using relevant feedback and control input templates taken from the CNN template library [Kék *et al.*, 2007] and [Chua & Yang, 1988a].

5.1.1. *Noise removal*

Let us consider as in [Chua & Yang, 1988a] a symmetric 2D DT-CNN for noise removal defined by the space-invariant feedback cloning template

$$\alpha = \begin{pmatrix} 0 & 1 & 0 \\ 1 & 2 & 1 \\ 0 & 1 & 0 \end{pmatrix} \in \mathbb{R}^{3\times 3}$$

the input (control) cloning template

$$\beta = \begin{pmatrix} 0 & 0 & 0 \\ 0 & 4 & 0 \\ 0 & 0 & 0 \end{pmatrix} \in \mathbb{R}^{3\times 3}$$

and $K = 0$.

Let $M = N = 20$. By explicitly computing with MATLAB the eigenvalues of T, we have $\lambda_{\min}(T) = -1.96$. Since T is not positive definite, we cannot use the result in [Chen & Shih, 2004] to establish convergence. However, we can apply Theorem 2. According to this theorem we have $\Theta_{2D} = -3$ and then $\eta_{\max} \geq 2/3$. Then, choose $\eta = 0.6 < \eta_{\max}$. Figure 15 depicts the initial image and the initial image with superimposed uniformly distributed noise within the interval $[-1, 1]$, the final image reached after convergence and one intermediate snapshot taken during the processing. Moreover, Fig. 16 depicts the states and outputs of the DT-CNNs, while Fig. 17 reports the behavior of the energy $W(x(k))$. In the figures, a white (resp., black) pixel corresponds to an output equal to $+1$ (resp., -1). Gray pixels correspond to intermediate output levels.

It is seen that, in accordance with Theorem 2 the DT-CNN is convergent and the energy is a decreasing function. Moreover, the DT-CNN is capable to effectively remove the noise superimposed on the initial image, with only two errors in the reconstruction of the image pixels.

It is worth to note that the estimate $\Theta_{2D} = -3$ obtained with Theorem 2 of $\lambda_{\min}(T - E_{400})$ is in good agreement with the actual value $\lambda_{\min}(T - E_{400}) = -2.96$ obtained with the explicit calculation with MATLAB of the eigenvalues of $T - E_{400}$.

5.1.2. *Hole filler*

Let us consider as in [Kék *et al.*, 2007] a symmetric 2D DT-CNN for filling the holes of an image defined

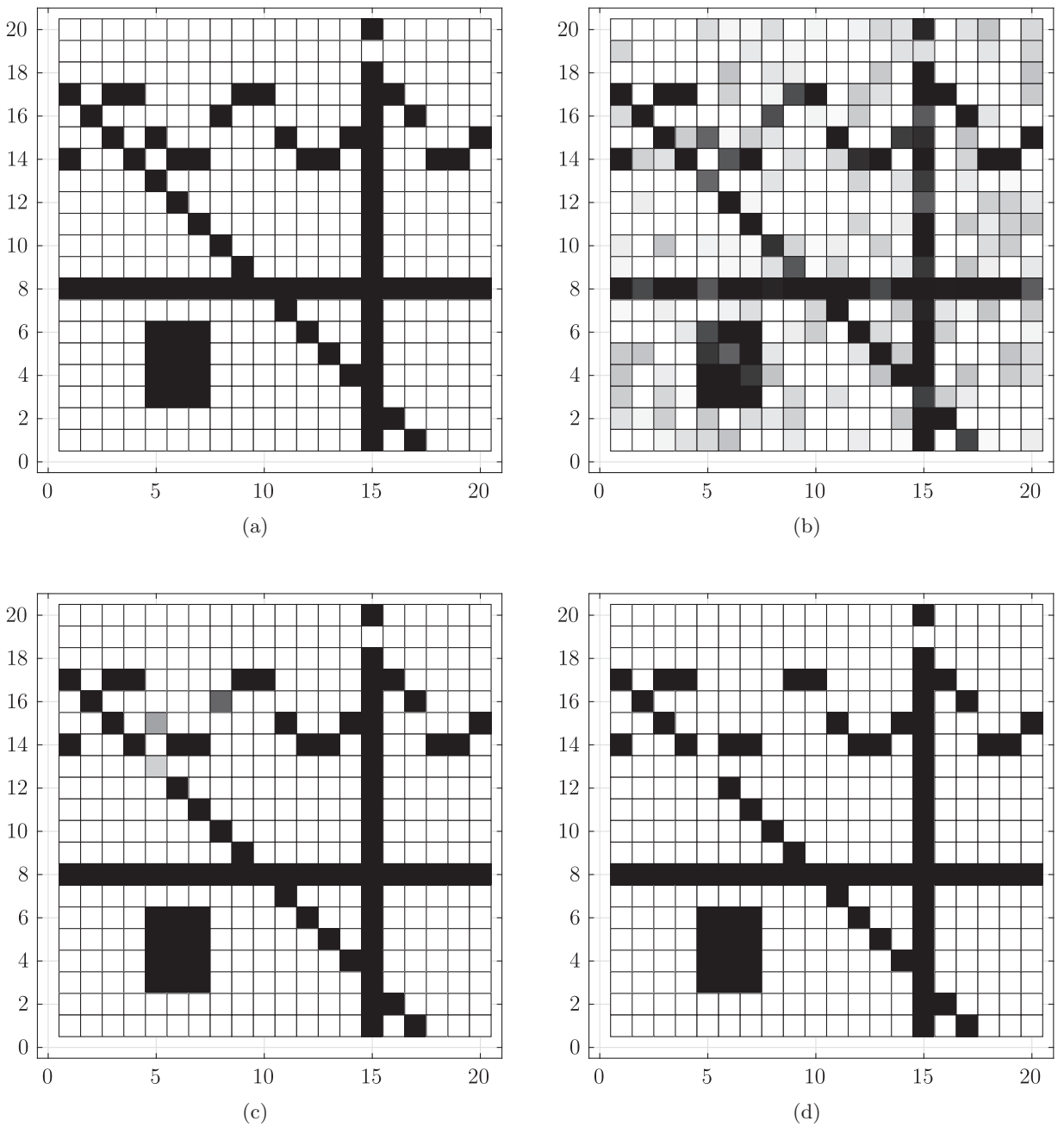

Fig. 15. 2D DT-CNN for noise removal. (a) Initial image, (b) initial image with superimposed noise, (c) intermediate snapshot at $k = 1$ and (d) final image after convergence.

by the space-invariant feedback cloning template

$$\alpha = \begin{pmatrix} 0 & 1.1 & 0 \\ 1.1 & 3 & 1.1 \\ 0 & 1.1 & 0 \end{pmatrix} \in \mathbb{R}^{3\times 3}$$

the input cloning template

$$\beta = \begin{pmatrix} 0 & 0 & 0 \\ 0 & 4 & 0 \\ 0 & 0 & 0 \end{pmatrix} \in \mathbb{R}^{3\times 3}$$

and $K = 1$.

Let $M = N = 20$. By explicitly computing with MATLAB the eigenvalues of T we have $\lambda_{\min}(T) = -1.35$. Since T is not positive definite, we cannot use the result in [Chen & Shih, 2004].

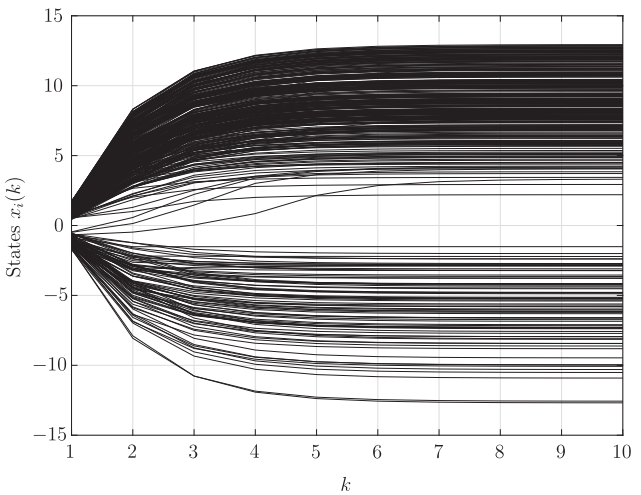

(a)

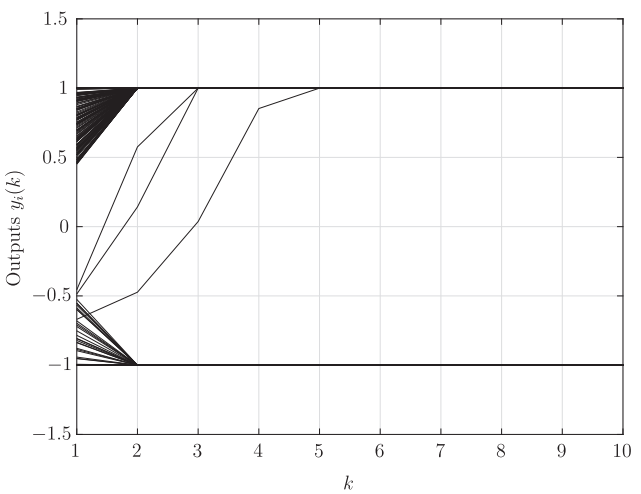

(b)

Fig. 16. (a) States and (b) outputs of DT-CNN for noise removal.

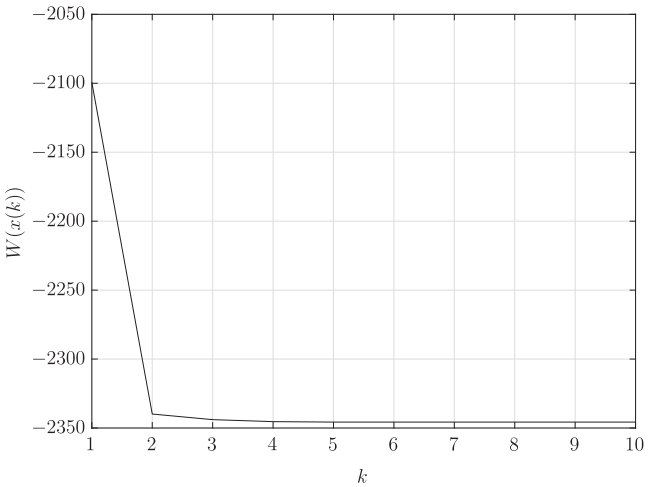

Fig. 17. Behavior of the energy of DT-CNN for noise removal.

However, we can apply Theorem 2, according to which $\Theta_{2D} = -2.4$ and $\eta_{\max} \geq 0.833$. Then, suppose that $\eta = 0.8 < \eta_{\max}$. Figure 18 depicts the initial image, the final image reached after convergence and two intermediate snapshots taken during the processing. Moreover, Fig. 19 depicts the states and outputs of the DT-CNNs, while Fig. 20 reports the behavior of the energy $W(x(k))$.

It is seen that, in accordance with Theorem 2 the DT-CNN is convergent and the energy is a decreasing function. Moreover, the holes of the given input image are correctly filled.

Also in this case the estimate $\Theta_{2D} = -2.4$ provided by Theorem 2 of $\lambda_{\min}(T - E_{400})$ is in good agreement with the actual value $\lambda_{\min}(T - E_{400}) = -2.351$ obtained with the explicit calculation by means of MATLAB of the eigenvalues of $T - E_{400}$.

5.1.3. *Patch maker*

Let us consider as in [Kék *et al.*, 2007] a symmetric 2D DT-CNN for patch making of an image defined by the space-invariant feedback cloning template

$$\alpha = \begin{pmatrix} 0 & 1 & 0 \\ 1 & 2 & 1 \\ 0 & 1 & 0 \end{pmatrix} \in \mathbb{R}^{3\times 3}$$

the input cloning template

$$\beta = \begin{pmatrix} 0 & 0 & 0 \\ 0 & 1 & 0 \\ 0 & 0 & 0 \end{pmatrix} \in \mathbb{R}^{3\times 3}$$

and $K = 30$.

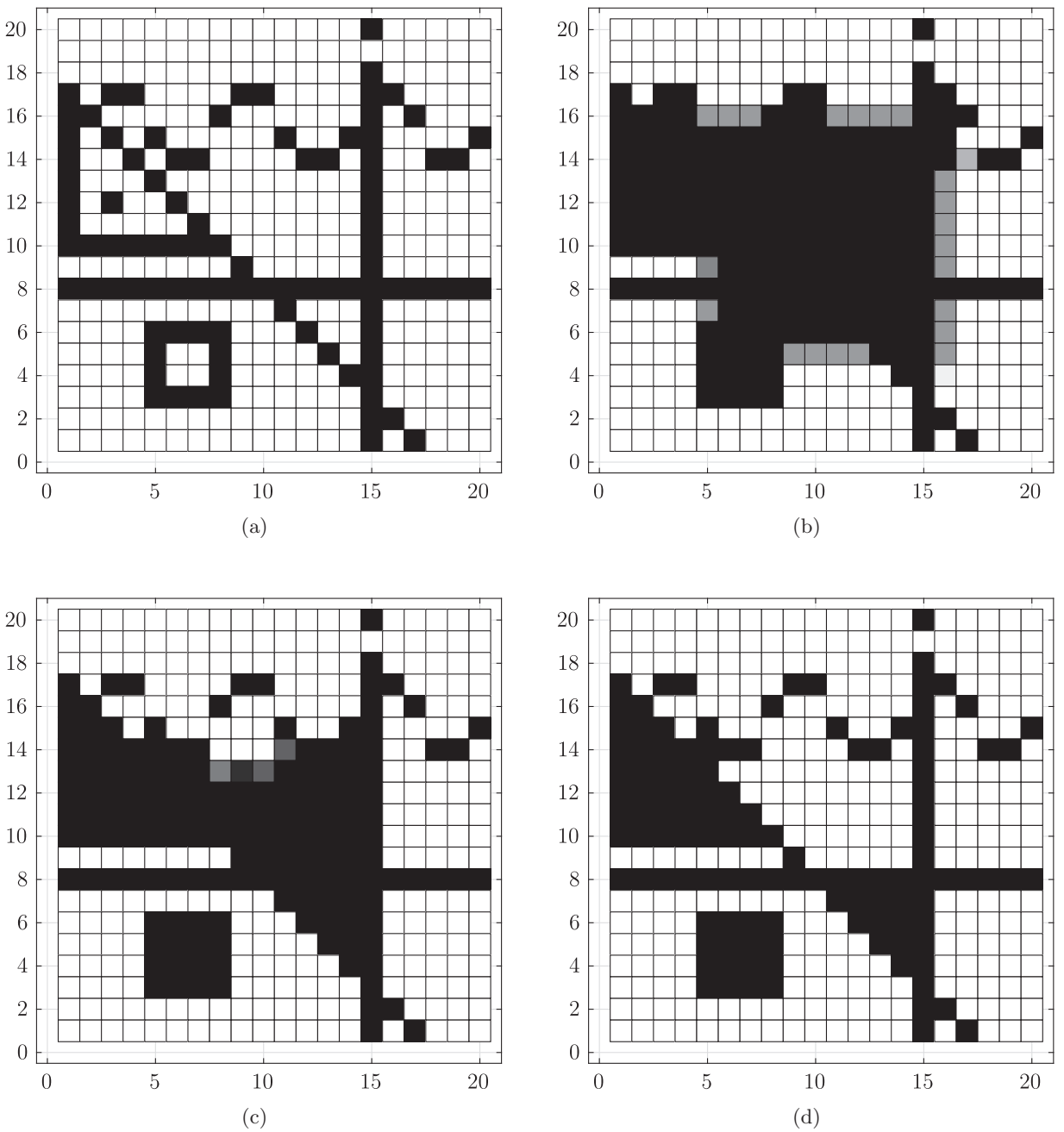

Fig. 18. Hole-filler 2D DT-CNN. (a) Initial image, (b) intermediate snapshot at $k = 9$, (c) intermediate snapshot at $k = 15$ and (d) final image after convergence.

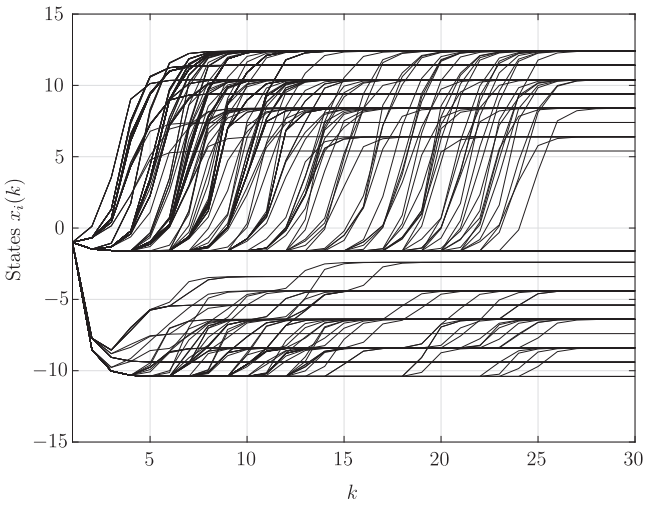

(a)

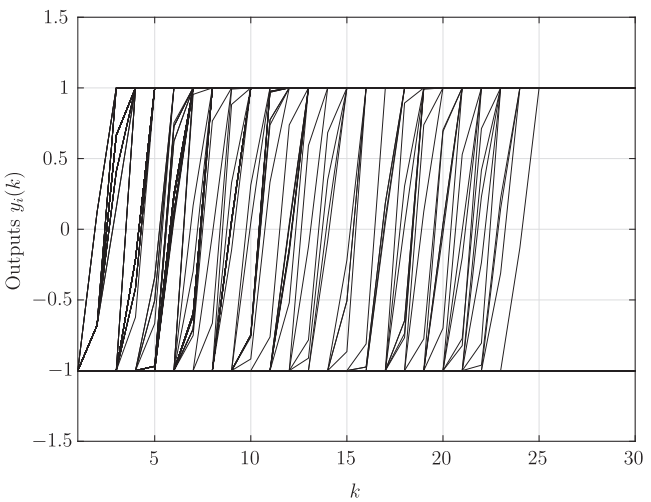

(b)

Fig. 19. (a) States and (b) outputs of hole-filler DT-CNN.

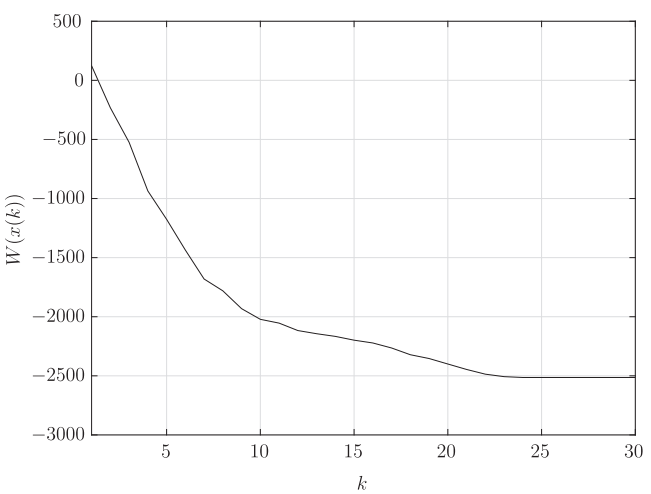

Fig. 20. Behavior of the energy of hole-filler DT-CNN.

Let $M = N = 20$. By explicitly computing with MATLAB the eigenvalues of T we have $\lambda_{\min}(T) = -1.96$. Since T is not positive definite, also in this case we cannot use the result in [Chen & Shih, 2004]. Nevertheless, Theorem 2 provides $\Theta_{2D} = -3$ and $\eta_{\max} \geq 2/3$. Then, choose $\eta = 0.6 < \eta_{\max}$. Figure 21 depicts the initial image, the final image reached after convergence and two intermediate snapshots taken during the processing. Moreover, Fig. 22 depicts the states and outputs of the DT-CNNs, while Fig. 23 reports the behavior of the energy $W(x(k))$.

It is seen that, in accordance with Theorem 2, the DT-CNN is convergent and the energy is a decreasing function. Moreover, the DT-CNN is able to effectively patch-make the given input image.

Again, the estimate $\Theta_{2D} = -3$ obtained with Theorem 2 of $\lambda_{\min}(T - E_{400})$ is in good agreement with the actual value $\lambda_{\min}(T - E_{400}) = -2.96$ obtained via MATLAB of the eigenvalues of $T - E_{400}$.

5.2. *1D DT-CNNs*

5.2.1. *Horizontal line detector*

Let us consider as in [Chua & Yang, 1988a] a symmetric 2D DT-CNN for horizontal line detection of an image with fixed boundary conditions. Actually, the DT-CNN cells are coupled only if they belong to the same image line. Therefore, we can describe their behavior via the 1D space-invariant feedback cloning template

$$\alpha = (1.6 \quad 2 \quad 1.6) \in \mathbb{R}^{1\times 3}$$

the input (control) cloning template $\beta = 0$ and $K = 1$.

Let $n = 25$. From (18) we have $\lambda_{\min}(T) = -1.196$. Since T is not positive definite, we cannot use the result in [Chen & Shih, 2004] to establish convergence. However, we can apply Theorem 4 obtaining $\eta_{\max} = 0.91$. Then, suppose that $\eta = 0.9 < \eta_{\max}$. Figure 24 depicts the initial image, the final image reached after convergence and one intermediate snapshot taken during the processing. Moreover, Fig. 25 depicts the states and outputs of the DT-CNNs, while Fig. 26 reports the behavior of the energy $W(x(k))$.

It is seen that, in accordance with Theorem 4 the DT-CNN is convergent and the energy is a decreasing function. Moreover, the horizontal lines of the given input image are correctly detected.

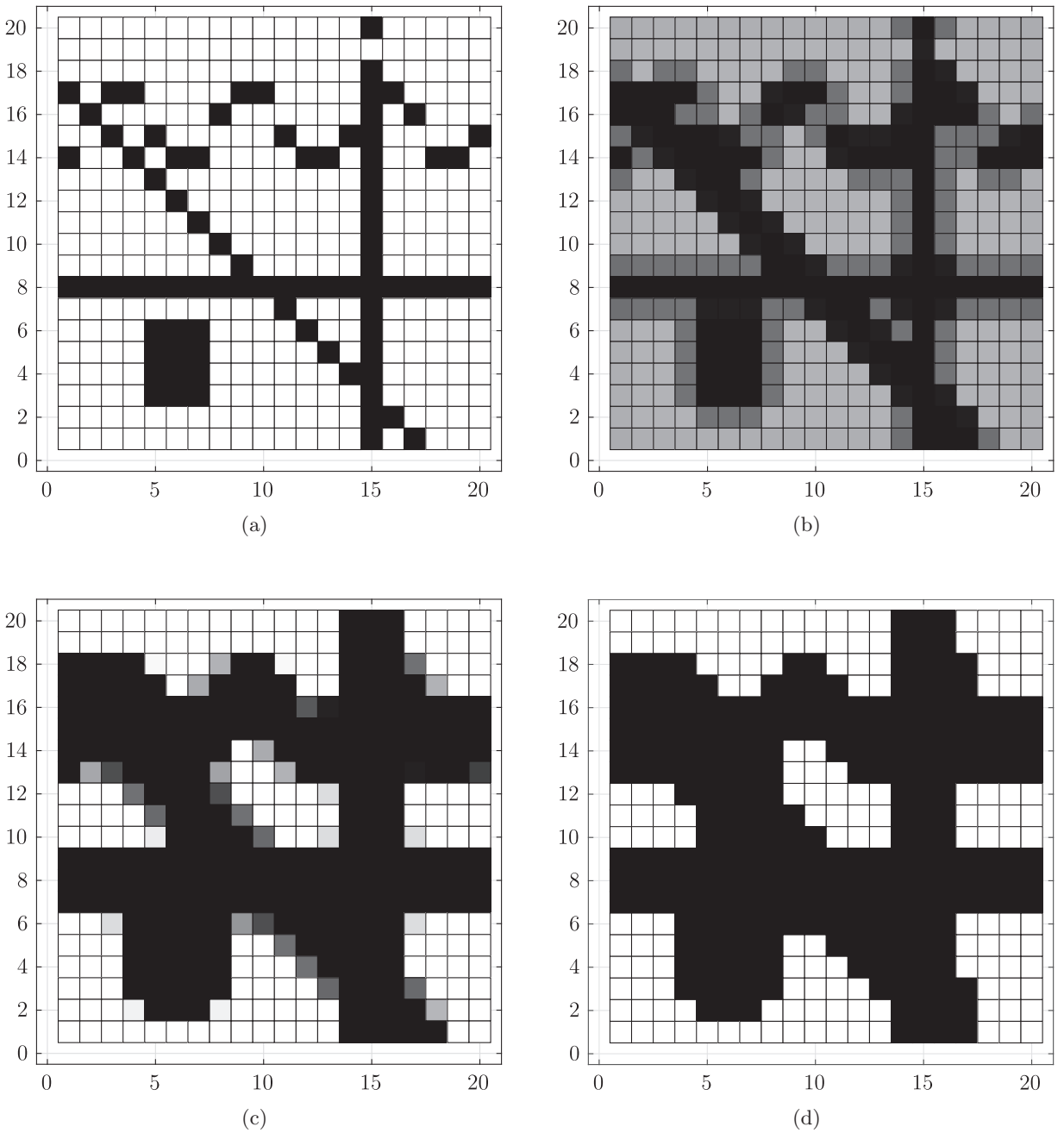

Fig. 21. Patch-maker 2D DT-CNN. (a) Initial image, (b) intermediate snapshot at $k = 3$, (c) intermediate snapshot at $k = 5$ and (d) final image after convergence.

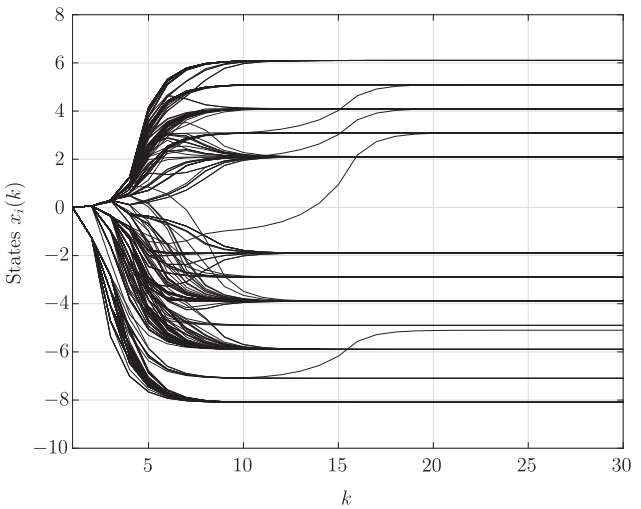

(a)

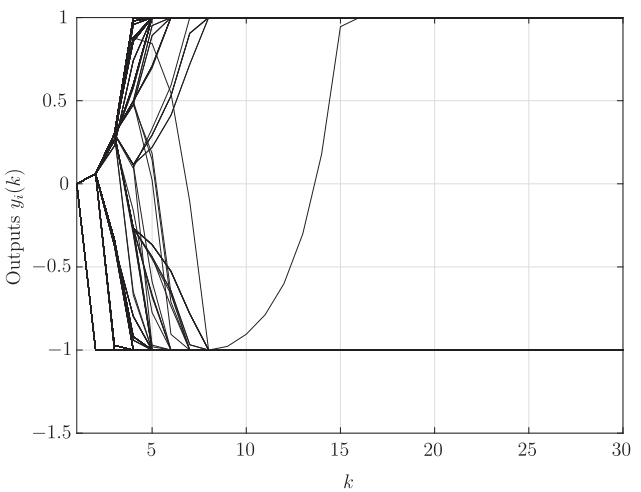

(b)

Fig. 22. (a) States and (b) outputs of patch-maker DT-CNN.

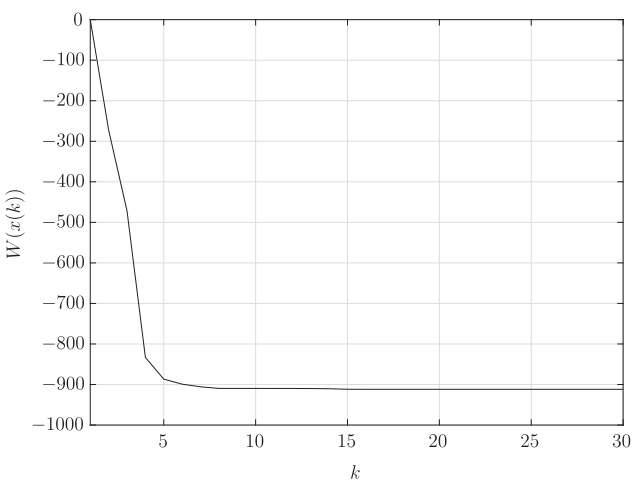

Fig. 23. Behavior of the energy of patch-maker DT-CNN.

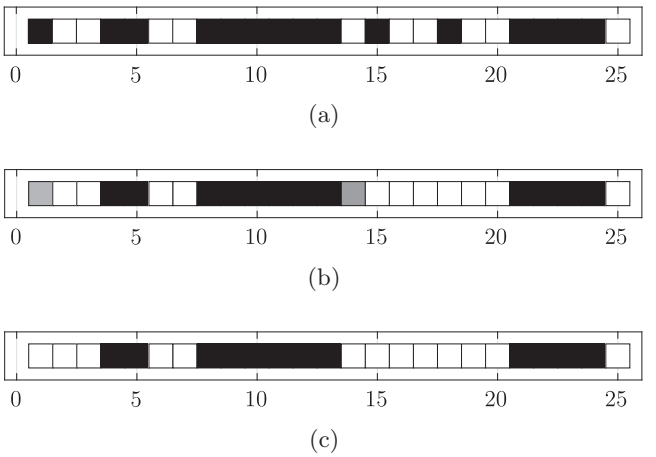

(a)

(b)

(c)

Fig. 24. 1D DT-CNN for horizontal line detection. (a) Initial image, (b) intermediate snapshot at $k = 1$ and (c) final image after convergence.

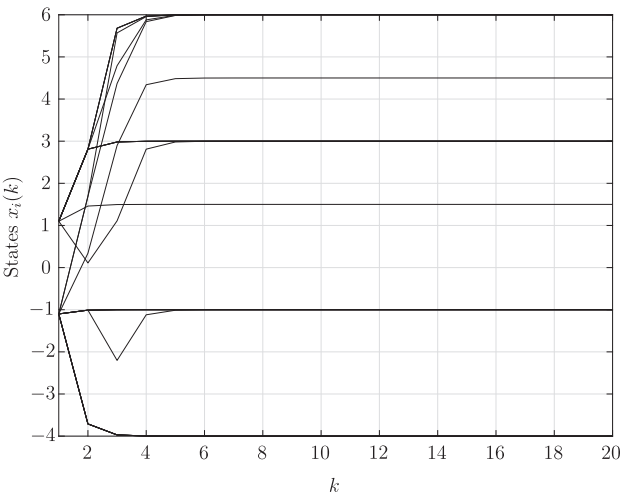

(a)

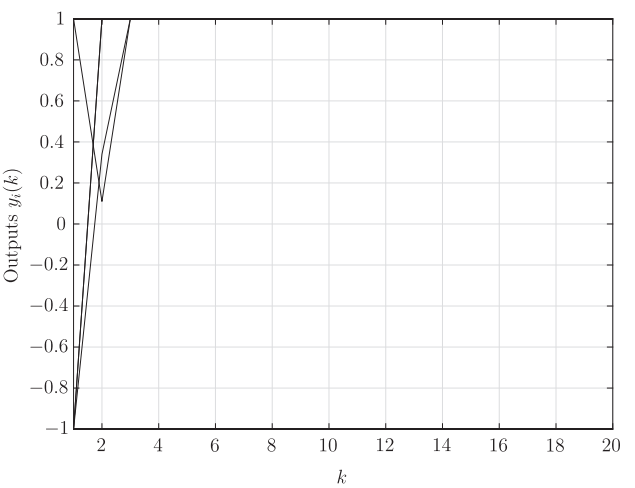

(b)

Fig. 25. (a) States and (b) outputs of DT-CNN for horizontal line detection.

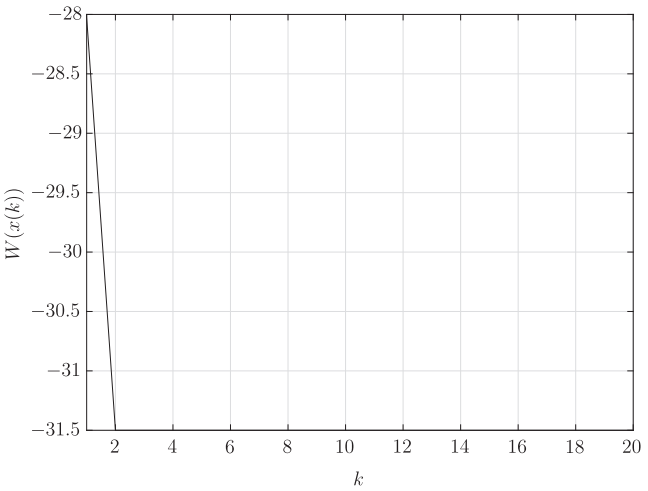

Fig. 26. Behavior of the energy of DT-CNN for horizontal line detection.

Finally, it is worth to note that the estimate (21), i.e. $-2.2 \leq \lambda_{\min}(T - E_{25})$, is in good agreement with the actual value $\lambda_{\min}(T - E_{25}) = -2.196$ obtained with the exact formula (18).

6. Conclusion

The paper has studied convergence of a class of synchronous DT-CNNs obtained by applying Euler's forward discretization scheme to standard CT-CNNs. The main result is that a DT-CNN is convergent if the interconnection matrix T is symmetric and, when $T + E_n$ is not positive semidefinite, the step size of discretization does not exceed a given bound. Notably, it is shown that the bound enjoys two key properties which follow from the local and space-invariant interconnection structure of a CNN. Namely, the bound is independent of the DT-CNN dimension and it can be easily evaluated as a function of the elements of the feedback template only. These properties make DT-CNNs very effective for computer simulations and high-dimension problems. The results are illustrated via the application of the DT-CNNs to image processing tasks. Future work will be devoted to study if the obtained convergence results can be extended to classes of DT-CNNs with nonsymmetric interconnections.

References

Anderson, J. A., Silverstein, J. W., Ritz, S. A. & Jones, R. S. [1977] "Distinctive features, categorical perception, and probability learning: Some applications of a neural model," *Psychol. Rev.* **84**, 413.

Arik, S. [2020] "New criteria for stability of neutral-type neural networks with multiple time delays," *IEEE Trans. Neur. Netw. Learn. Syst.* **31**, 1504–1513.

Brucoli, M., Carnimeo, L. & Grassi, G. [1995] "Discrete-time cellular neural networks for associative memories with learning and forgetting capabilities," *IEEE Trans. Circuits Syst.-I*: *Fund. Th. Appl.* **42**, 396–399.

Chen, S.-S. & Shih, C.-W. [2004] "Dynamics for discrete-time cellular neural networks," *Int. J. Bifurcation and Chaos* **14**, 2667–2687.

Chen, W.-H., Lu, X. & Zheng, W. X. [2014] "Impulsive stabilization and impulsive synchronization of discrete-time delayed neural networks," *IEEE Trans. Neur. Netw. Learn. Syst.* **26**, 734–748.

Cheng, C.-Y., Lin, K.-H. & Shih, C.-W. [2006] "Multistability in recurrent neural networks," *SIAM J. Appl. Math.* **66**, 1301–1320.

Chua, L. O. & Yang, L. [1988a] "Cellular neural networks: Applications," *IEEE Trans. Circuits Syst.* **35**, 1273–1290.

Chua, L. O. & Yang, L. [1988b] "Cellular neural networks: Theory," *IEEE Trans. Circuits Syst.* **35**, 1257–1272.

Chua, L. O., Hasler, M., Moschytz, G. S. & Neirynck, J. [1995] "Autonomous cellular neural networks: A unified paradigm for pattern formation and active wave propagation," *IEEE Trans. Circuits Syst.-I*: *Fund. Th. Appl.* **42**, 559–577.

Chua, L. O. & Roska, T. [2005] *Cellular Neural Networks and Visual Computing*: *Foundation and Applications* (Cambridge University Press).

Ciarlet, P. G. [2013] *Linear and Nonlinear Functional Analysis with Applications*, Vol. 130 (SIAM Press).

Cohen, M. A. & Grossberg, S. [1983] "Absolute stability of global pattern formation and parallel memory storage by competitive neural networks," *IEEE Trans. Syst. Man Cybern.* **13**, 815–825.

Corinto, F. & Gilli, M. [2003] "Comparison between the dynamic behaviour of Chua–Yang and full-range cellular neural networks," *Int. J. Circuit Th. Appl.* **31**, 423–441.

Davis, P. J. [2012] *Circulant Matrices* (Amer. Math. Soc.).

Di Marco, M., Forti, M., Grazzini, M. & Pancioni, L. [2010] "Limit set dichotomy and convergence of semiflows defined by cooperative standard CNNs," *Int. J. Bifurcation and Chaos* **20**, 3549–3563.

Di Marco, M., Forti, M., Grazzini, M. & Pancioni, L. [2011] "Limit set dichotomy and convergence of cooperative piecewise linear neural networks," *IEEE Trans. Circuits Syst.-I*: *Reg. Papers* **58**, 1052–1062.

Di Marco, M., Forti, M., Grazzini, M. & Pancioni, L. [2012a] "Convergence of a class of cooperative standard cellular neural network arrays," *IEEE Trans. Circuits Syst.-I*: *Reg. Papers* **59**, 772–783.

Di Marco, M., Forti, M., Grazzini, M. & Pancioni, L. [2012b] "Limit set dichotomy and multistability for a class of cooperative neural networks with delays," *IEEE Trans. Neur. Netw. Learn. Syst.* **23**, 1473–1485.

Ding, S. & Wang, Z. [2020] "Event-triggered synchronization of discrete-time neural networks: A switching approach," *Neur. Netw.* **125**, 31–40.

Espejo, S., Carmona, R., Domínguez-Castro, R. & Rodríguez-Vázquez, A. [1996] "A VLSI oriented continuous time CNN model," *Int. J. Circuit Th. Appl.* **24**, 341–356.

Forti, M. & Tesi, A. [2001] "A new method to analyze complete stability of PWL cellular neural networks," *Int. J. Bifurcation and Chaos* **11**, 655–676.

Forti, M. & Tesi, A. [2004] "Absolute stability of analytic neural networks: An approach based on finite trajectory length," *IEEE Trans. Circuits Syst.-I*: *Reg. Papers* **51**, 2460–2469.

Golden, R. M. [1986] "The brain-state-in-a-box neural model is a gradient descent algorithm," *J. Math. Psychol.* **30**, 73–80.

Hänggi, M. & Moschytz, G. S. [2000] *Cellular Neural Networks*: *Analysis*, *Design and Optimization* (Springer Science & Business Media).

Harrer, H. & Nossek, J. A. [1992] "Discrete-time cellular neural networks," *Int. J. Circuit Th. Appl.* **20**, 453–467.

Harrer, H., Nossek, J. A. & Stelzl, R. [1992] "An analog implementation of discrete-time cellular neural networks," *IEEE Trans. Neur. Netw.* **3**, 466–476.

Haykin, S. [1999] *Neural Networks*: *A Comprehensive Foundation* (Prentice-Hall).

Hirsch, M. W. [1982] "Systems of differential equations which are competitive or cooperative. I: Limit sets," *SIAM J. Math. Anal.* **13**, 167–179.

Hirsch, M. W. [1989] "Convergent activation dynamics in continuous time networks," *Neur. Netw.* **2**, 331–349.

Hopfield, J. J. [1982] "Neural networks and physical systems with emergent collective computational abilities," *Proc. Natl. Acad. Sci.* **79**, 2554–2558.

Hopfield, J. J. [1984] "Neurons with graded response have collective computational properties like those of two-state neurons," *Proc. Natl. Acad. Sci.* **81**, 3088–3092.

Johnson, L. W., Riess, R. D. & Arnold, J. T. [1993] *Introduction to Linear Algebra* (Addison Wesley).

Kék, L., Karacs, K. & Roska, T. [2007] "Cellular wave computing library (templates, algorithms, and programs). Version 2.1," *Research Report of Cellular Sensory and Wave Computing Laboratory CSW-1-2007.*

Mei, W. & Bullo, F. [2017] "LaSalle invariance principle for discrete-time dynamical systems: A concise and self-contained tutorial," arXiv preprint arXiv: 1710.03710.

Michel, A. N., Farrell, J. A. & Porod, W. [1989] "Qualitative analysis of neural networks," *IEEE Trans. Circuits Syst.* **36**, 229–243.

Michel, A. N., Si, J. & Yen, G. [1991] "Analysis and synthesis of a class of discrete-time neural networks described on hypercubes," *IEEE Trans. Neur. Netw.* **2**, 32–46.

Roska, T., Arena, P. & Rekeczky, C. (eds.) [2006] "Special issue on CNN technology (Part 1)," *Int. J. Circuit Th. Appl.* **34**.

Roska, T., Arena, P., Lin, C.-T. & Tetzlaff, R. (eds.) [2009] "Special issue on cellular wave computing architecture," *Int. J. Circuit Th. Appl.* **37**.

Shi, B. E., Arena, P. & Zarandy, A. (eds.) [2004] "Special issue on CNN technology and active wave computing," *IEEE Trans. Circuits Syst.-I*: *Fund. Th. Appl.* **51**.

Thiran, P., Crounse, K. R., Chua, L. O. & Hasler, M. [1995] "Pattern formation properties of autonomous cellular neural networks," *IEEE Trans. Circuits Syst.-I*: *Fund. Th. Appl.* **42**, 757–774.

Yang, S., Liu, Q. & Wang, J. [2018] "A collaborative neurodynamic approach to multiple-objective distributed optimization," *IEEE Trans. Neur. Netw. Learn. Syst.* **29**, 981–992.

Zurada, J. [1992] *Introduction to Artificial Neural Systems* (West Publ.).